

Vorinostat potentiates vesicular stomatitis virus oncolysis by modulating autophagy in an NF- κ B-dependent manner

A thesis submitted to McGill University in partial fulfillment of the requirements of the degree of Master of Science

by

Laura Shulak

Division of Experimental Medicine, Department of Medicine, McGill University,
Montreal, Quebec, Canada

December 2013

©Laura Shulak 2013

Abstract

Vesicular stomatitis virus (VSV) replication and oncolytic potential is reversibly stimulated in combination with epigenetic modulators such as the histone deacetylase inhibitor (HDI) Vorinostat (SAHA). Based on this reversible effect of Vorinostat on viral oncolysis, we reasoned that critical host genes involved in oncolysis may be reversibly regulated in prostate cancer PC3 cells following removal of Vorinostat. A transcriptome analysis in PC3 cells identified a subset of NF- κ B target genes that were reversibly regulated by Vorinostat and involved in regulation of inflammatory and stress-responses. Consistent with the induction of NF- κ B target genes, Vorinostat-mediated enhancement of VSV oncolysis correlated with hyper-acetylation of the NF- κ B transcription factor subunit RELA/p65; furthermore, VSV replication and cell killing were suppressed when NF- κ B signaling was inhibited using pharmacological or genetic approaches. Additional bioinformatics analysis revealed that stimulation of NF- κ B signaling also resulted in the increased expression of several autophagy-related genes. Inhibition of autophagy by 3-methyladenine led to an increase in expression of IFN β -stimulated genes, and both 3-methyladenine treatment and genetic ablation of autophagy led to a decrease in VSV replication and oncolysis. Together, these data demonstrate that Vorinostat stimulates NF- κ B activity in a reversible manner via modulation of RelA/p65 signaling, leading to induction of autophagy and enhancement of VSV replication and oncolysis. These studies thus positively correlate NF- κ B signaling and autophagy with VSV replication and oncolysis.

Résumé

La réplication et l'activité oncolytique du virus de la stomatite vésiculaire (VSV) sont stimulées d'une manière réversible lorsque le VSV est combiné avec des modulateurs épigénétiques tels que le vorinostat (SAHA), un inhibiteur de l'histone déacétylase (IDH). En se basant sur cette observation, nous avons émis l'hypothèse que les gènes importants de l'hôte impliqués dans l'oncolyse peuvent-être eux aussi réversiblement régules dans les cellules du cancer de la prostate PC3 après le retrait du vorinostat. En effet, une analyse du transcriptome des cellules PC3 a identifié un set de gènes impliqués dans la voie NF- κ B, plus précisément dans la réponse inflammatoire et aux réponses au stress, qui est régulé par le vorinostat. Conformément à l'induction des gènes cibles de la voie NF- κ B, l'amélioration de l'effet oncolytique du VSV par le vorinostat corrèle avec une hyperacétylation du NF- κ B RELA/p65; En outre, la réplication du VSV et la mort des cellules ont été supprimées lorsque la voie signalétique NF- κ B a été inhibée par des approches pharmacologiques et géniques. Nous avons également observé que l'expression de plusieurs gènes impliqués dans l'autophagie a été augmentée par la stimulation de la voie NF- κ B. De plus, une analyse supplémentaire bioinformatique a révélé que l'expression de plusieurs gènes impliqués dans l'autophagie était également augmentée par la stimulation de NF- κ B. En addition, l'inhibition de l'autophagie par le 3-méthyladénine a entraîné une amplification de l'expression des gènes stimulés par l'IFN- β . En outre, le traitement avec le 3-méthyladénine et l'inhibition génique de l'autophagie a résulté en une diminution de la réplication du VSV et de l'oncolyse. Ensemble, ces résultats démontrent que le vorinostat stimule l'activité du NF- κ B de manière réversible via la modulation de RelA/p65, conduisant à l'induction de l'autophagie et à l'amélioration de la réplication du

VSV et l'oncolyse. Ainsi, cette étude met en évidence le lien entre l'activation de l'axe NF-kB- autophagie et la réplication du VSV et son effet oncolytique.

Acknowledgements

In completing my Master's thesis project, I would first like to thank my supervisors, Dr. John Hiscott and Dr. Rongtuan Lin, for giving me the opportunity to complete my project in their excellent laboratory. Their patience, guidance and encouragement have been greatly appreciated throughout my project, and I am truly grateful to have had them as my co-supervisors.

In addition, I would like to thank all of the past and present members of the Hiscott/Lin lab for all of their support and company in my three years in the lab. I would specifically like to acknowledge Dr. Thi Lien-Anh Nguyen for teaching me basically everything I know about how to function in a lab, and for her help in conceiving my project. I'd like to thank Drs. S. Mehdi Belgnaoui and Suzanne Paz for their patience and encouragement and input in my experiments. I'd like to thank Dr. Julien van Grevenynghe for his help with the flow cytometry experiments, and Dr. Vladimir Beljanski for his help with writing and editing the manuscript. Dr. Sara Samuel, Dr. Fethia Ben-Yebdri, Dr. Simon Leveille, Marie-Line Goulet and Samar bel-Hadj for their support and advice. Finally my friend and labmate Alexandre Sze, whom I pestered to join the lab and who has been an indispensable source of moral support.

I am forever grateful to my family and friends for their full support and love throughout my graduate studies. Their motivation and reassurance was crucial.

Preface

In accordance with the “Guidelines for Thesis preparation”, this thesis is presented in a Manuscript-based format. A general introduction precedes the results chapter:

Manuscript I

Histone deacetylase inhibitors potentiate VSV oncolysis in prostate cancer cells by modulating NF- κ B signaling

This manuscript is currently in preparation for submission to the Journal of Virology.

Laura Shulak¹, Vladimir Beljanski², Cindy Chiang², Sucharita M. Dutta³, Julien Van Grevenynghe¹, S. Mehdi Belgnaoui¹, Thi Lien-Anh Nguyen¹, Thomas Di Lenardo¹, Rongutan Lin¹, O. John Semmes³, and John Hiscott²

Contribution of the authors

LS conceived, designed, performed experiments, microarray data analysis, and wrote the manuscript. VB performed experiments and wrote the manuscript. CC, JVG and TD performed experiments. SD performed and analyzed MS experiments. SMB edited the manuscript. TLN conceived experiments. RL generated S-tagged RelA/p65 vector. OJS collaborated in MS. JH wrote the manuscript and JH and RL supervised study.

Table of Contents

TITLE PAGE.....	1
ABSTRACT	2
RÉSUMÉ	3
ACKNOWLEDGEMENTS	5
PREFACE	6
TABLE OF CONTENTS.....	7
LIST OF FIGURES AND TABLES	9
LIST OF ABBREVIATIONS	10
CHAPTER 1 INTRODUCTION	12
1.1 Prostate Cancer	14
1.1.1. Prostate Cancer Therapy	14
1.2 Oncolytic Viruses (OVs).....	15
1.2.1 Molecular basis for cancer specificity of oncolytic viruses.....	16
1.2.2 Desirable characteristics of oncolytic viruses & therapeutic efficacy.....	18
1.3 Vesicular stomatitis virus (VSV) Virology.....	20
1.3.1 VSV Pathogenesis: molecular and cellular basis.....	23
1.3.2 VSV as an Oncolytic Virus.....	24
1.3.3 VSV combination treatment strategies.....	26
1.4 Histone deacetylase inhibitors.....	27
1.4.1 Mechanisms of HDI-mediated enhancement of OV therapy.....	28
1.5 NF- κ B signaling.....	29
1.5.1 Role of NF- κ B in viral infections.....	30
1.5.2 Cross-talk between NF- κ B and autophagy.....	31
1.6 Autophagy.....	32
1.6.1 Autophagy & viral infections.....	33
1.6.2 Autophagy & cancer.....	34
References.....	35
CHAPTER 2 RESULTS	46

Manuscript I	47
---------------------------	-----------

Histone deacetylase inhibitors potentiate VSV oncolysis in prostate cancer cells by modulating NF- κ B signaling

Rationale for Manuscript I	48
Abstract.....	49
Introduction.....	50
Results	53
Discussion	73
Materials and Methods	79
References	87

CHAPTER 3 DISCUSSION	92
-----------------------------------	-----------

3.1 Oncolytic virotherapy.....	93
3.2 Vorinostat stimulates NF-κB signaling and target gene upregulation.....	94
3.3 VSV oncolysis of prostate cancer cells requires induction of autophagy....	96
2.4 Concluding remarks.....	96

References.....	98
------------------------	-----------

List of Figures and Tables

CHAPTER 2 RESULTS

Manuscript I- Histone deacetylase inhibitors potentiate VSV oncolysis in prostate cancer cells by modulating NF- κ B signaling

Figure 1: Vorinostat treatment-induced expression of NF- κ B regulated genes...

Figure 2: Continuous HDI treatment leads to hyperacetylation and increased DNA binding of RelA/p65.....

Figure 3: NF- κ B inhibition blocks Vorinostat-induced RelA/p65 nuclear translocation and target gene expression.....

Figure 4: Inhibition of NF- κ B signaling blocks Vorinostat-mediated enhancement of VSV replication in PC3 cells

Figure 5: Inhibition of NF- κ B signaling blocks Vorinostat-mediated enhancement of VSV replication in other refractory cells

Figure 6: Vorinostat treatment stimulates autophagy in an NF- κ B-dependent manner...

Figure 7: Inhibition of autophagy suppresses VSV replication.

Figure 8: A proposed model of Vorinostat-mediated enhancement of VSV oncolysis....

List of abbreviations

APC	Allophycocyanin
AR	Androgen receptor
ATF-2/c-Jun	Activating Transcription Factor 2
Atg	Autophagy related gene
Bax	Bcl-2-associated X protein
Bcl-2	B-cell lymphoma 2
BIRC3	Baculoviral IAP (inhibitor of apoptosis) repeat containing 3
CAB	Combined androgen blockade
CAR	Coxsackie and adenovirus receptor
CARD	Caspase recruitment domain
CDKN1A	Cyclin-dependent kinase inhibitor 1A (p21)
CTCF	Calculated total cell fluorescence
CTCL	Cutaneous T-cell lymphoma
DNA	Deoxyribonucleic acid
ER	Endoplasmic reticulum
G	Glycoprotein
GFP	Green fluorescent protein
GM-CSF	Granulocyte-Macrophage Colony Stimulating Factor
IFN	Interferon
IFNAR	Interferon alpha/beta receptor
I κ B	Inhibitor of κ B
IKK	Inhibitor of κ B kinase
IL-6	Interleukin-6
IPS-1	IFN β promoter stimulator I
IRF	Interferon regulatory factor
IRF3	Interferon regulatory factor 3
ISG	Interferon stimulated gene
HAT	Histone acetyltransferase
HDAC	Histone deacetylase

HDI	Histone deacetylase inhibitor
HSV	Herpes simplex virus
JAK/STAT	Janus Kinase/Signal Transducer and Activator of Transcription
OV	Oncolytic virus
L	Large polymerase protein
LDL	Low-density lipoprotein
LHRH	Luteinizing hormone-releasing hormone
M	Matrix protein
MEF	Mouse embryonic fibroblast
MFI	Mean fluorescence intensity
MOI	Multiplicity of infection
mRNA	Messenger RNA
mTOR	Mammalian target of rapamycin
N	Nucleocapsid protein
NAD	Nicotinamide adenine dinucleotide
NEMO	NF- κ B essential modulator
NF- κ B	Nuclear factor kappa-light-chain-enhancer of activated B cells
NLS	Nuclear localisation signal
P	Phosphoprotein
PCa	Prostate cancer
PKR	Double-stranded-RNA-dependent protein kinase
P53	Tumor protein 53
Ras	Small GTPase
RdRp	RNA dependent RNA polymerase
RHD	Rel homology domain
RIG-I	Retinoic acid-inducible I
RLR	Retinoic acid-inducible I-like receptor
RNA	Ribonucleic acid
RNP	Ribonucleoprotein
shRNA	Short hairpin RNA
TAD	Transactivation domain
TAK1	TGF β -activating kinase
TNFAIP3	Tumor necrosis factor alpha induced protein 3 (A20)

VSV	Vesicular stomatitis virus
WT	Wild-type
3MA	3-methyladenine

CHAPTER 1

INTRODUCTION

1.1 Prostate Cancer

Prostate cancer (PCa) is the most commonly diagnosed non-cutaneous malignancy in Western males and the second leading cause of cancer-related deaths in men worldwide (Drake, 2010; Shen and Abate-Shen, 2010). The American Cancer Society estimates that in 2013, approximately 238,590 men will be diagnosed with PCa and that 29,720 will die from PCa related causes (Siegel *et al.*, 2013). Though PCa can grow slowly and locally for many years, it eventually reaches neighbouring tissues or metastasizes to distant ones, most commonly the lungs, liver, and bone (Bubendorf *et al.*, 2000). Classification of PCa is based on the TNM (tumor, nodes, metastasis) system, which describes the size of the primary tumor, involvement of regional lymph nodes, and whether metastatic dissemination has occurred. This system may also be combined with tumor grading by the Gleason scoring system, which generally ranges from 2 to 10 (Borley and Feneley., 2009).

1.1.1 Prostate Cancer Therapy

Initially, locally advanced PCa is hormone-sensitive and the first treatment is hormone therapy, more specifically, androgen-deprivation therapy (Tadros and Garzotto, 2011). The primary androgens are testosterone and the more active metabolite dihydrotestosterone, which are produced in the testes and trigger prostate cancer cell growth. The androgens bind and transactivate the androgen receptor (AR), which interacts with various co-factors to mediate gene expression during PCa progression. Reducing androgen levels or inhibiting AR binding diminishes the growth rate of the

tumor. Androgen deprivation therapy constitutes surgical castration, medical castration with luteinizing hormone-releasing hormone (LHRH) agonist therapy, or inhibitory anti-androgen drugs (Ziparo *et al.*, 2013). The use of the latter is usually combined with either surgical or medical castration as first-line treatment, termed “combined androgen blockade” (CAB). Though androgen deprivation therapy is initially successful in suppressing tumor growth, it eventually fails. This leads to the evolution of hormone-refractory (or androgen-independent) PCa, where tumor growth is recurrent and no longer sensitive to castration. Androgen independence is largely responsible for the morbidity and mortality attributed to PCa (Drake, 2010). When patients reach this state and begin to show symptoms of metastasis, other treatment strategies must be initiated.

In addition to radiation therapy, various small molecule-based therapies have been utilized in treatments (Shen and Abate-Shen, 2010; Yap *et al.*, 2011; Wilkins and Parker, 2010). To date, only a few therapeutic options exist for the treatment of hormone-refractory PCa and their efficiency is short-lived, thus reflecting an unmet need for novel, more effective treatments.

1.2 Oncolytic Viruses

Viruses represent a unique class of organisms. Though they possess genes, replicate their DNA, and evolve through natural selection, ultimately, their survival and propagation depends on efficiently hijacking host cells. Consequentially, both the host and the virus have developed mutually responsive systems in an attempt to “one-up” the other. Hosts have evolved complex immune systems to thwart infection, while viruses possess a myriad of strategies to circumvent these systems, or even appropriate them to their own advantage. When the host’s immune system is compromised, for example in

immunosuppressed HIV or post-transplant patients, this provides a breeding ground for opportunistic viral infections.

Inherent cellular deregulation can also lead to immune deregulation, a notable example being cancer. Case reports demonstrating the anti-tumor effect of naturally acquired viral infections date back to the mid-19th century, before viruses were even identified (Kelly *et al.*, 2007). Over the years, there have been a number of cases reporting cancer remission concomitant with viral infection. Several patients with hematological malignancies experienced tumor regression following natural measles and influenza infections (Pasquinucci, 1971; Taqi *et al.*, 1981; Bluming and Ziegler, 1971). Such cases led to the recognition of the therapeutic potential of oncolytic viruses (OVs), creating a novel research field that has grown significantly in the past few decades. The basic tenet is that the genetic abnormalities and altered signaling pathways conferring growth and survival advantages to cancer cells have a tendency to give way to reduced immune functioning. OVs take advantage of these features, and are able to infect, replicate in, and kill these cells. Normal cells however, with intact cell cycles and antiviral responses, clear the infection with minimal damage.

1.2.1 Molecular basis for cancer specificity of oncolytic viruses

Cancer cells are characterized by six distinct, requisite changes in cell physiology (Hanahan and Weinberg, 2000):

- 1) Self-sufficiency in growth signals
- 2) Insensitivity to growth-inhibitory signals

- 3) Apoptosis (programmed cell death) evasion
- 4) Limitless replicative potential
- 5) Sustained angiogenesis
- 6) Ability to invade tissue and metastasize

These changes are generally achieved by an accumulation of genetic and epigenetic mutations that give way to new metabolic phenotypes, allowing the transformed cells to produce sufficient energy for constitutive proliferation while avoiding checkpoint controls which would, under normal circumstances, inhibit uncontrolled growth (Cairns, *et al.*, 2011). Cell death pathways, such as apoptosis, autophagy, and necrosis, are often suppressed in cancer cells (Elmore, 2007; Hanahan and Weinberg, 2000; Ouyang *et al.*, 2012; Pattingre and Levine, 2006), and immune evasion strategies are commonly used to favor tumor survival (Critchley-Thorne *et al.*, 2009; Mapara and Sykes, 2004). These alterations play a key role in tumor cells' susceptibility to OVIs, since cell death and growth signals are closely linked to antiviral and interferon (IFN) responses such as the Janus Kinase/Signal Transducer and Activator of Transcription (JAK/STAT) pathway. Activation of this pathway is largely responsible for amplification of the antiviral state and also controls cell survival and proliferation (Constantinescu *et al.*, 2008). IFN signaling also mediates several p53-regulated anti-tumor and antiviral responses (Takaoka *et al.*, 2003). p53, a tumor suppressor protein involved in cell cycle arrest and apoptosis, is one of the most commonly mutated genes in human cancers (Hollstein *et al.*, 1991). Another example of convergent IFN and apoptotic signaling can be seen in the dual regulatory role of interferon regulatory factor 3 (IRF3) transcription factor, which upon viral infection, is essential in initiating both the type I IFN response and cell death via activation of the pro-apoptotic Bcl-2-associated X protein (Bax)

(Chattopadhyay *et al.*, 2010). Over-activation of the Ras signaling pathway, which regulates proliferation, survival, and differentiation, is a frequent occurrence in tumor cells, and has been shown to inhibit the antiviral activity of IFN α by reducing STAT2 levels (Downward, 2003; Christian *et al.*, 2009). While modulation of these pathways confers a survival advantage to cancers, they also create an environment that is favorable to viral replication. OV's are thus able to exploit these changes to preferentially infect, replicate in, and kill tumor cells.

1.2.2 Desirable characteristics of oncolytic viruses & therapeutic efficacy

A number of naturally occurring and genetically engineered viruses have been utilized in oncolytic virotherapy. Both RNA viruses (such as Vesicular stomatitis virus (VSV), Newcastle disease virus, Reovirus, and Measles virus) and DNA viruses (such as Adenovirus, Vaccinia virus, and Herpes simplex virus (HSV)) have been used with varying degrees of success. Ideally, an OV should possess as many of the following properties as possible (Parato *et al.*, 2005):

- 1) Cancer specificity (selective targeting and lysing of cancer cells)
- 2) Broad tropism of tumor cells and cancer types
- 3) Sensitivity to host antiviral response in normal cells
- 4) Non-pathogenic to limit adverse effects and toxicity in normal cells
- 5) Strictly cytoplasmic replication and inability to integrate into host genome
- 6) Rapid replication, lysis, and viral spread
- 7) Efficient tumor delivery through systemic route

Though OV's have been in clinical trials since the 1950s, today the number of trials has expanded significantly, with a several entering phase III. In 2005, H101, an Adenovirus which preferentially replicates in p53-mutant cells, was the first replication-competent OV approved for head and neck cancer treatment in China (Garber, 2006). A recent trial in melanoma patients using OncoVEX^{GM-CSF}, an HSV-1 virus possessing deletions in its' virulence factor genes in addition to expression of Granulocyte-Macrophage Colony Stimulating Factor (GM-CSF), has exhibited clinical efficacy. In a phase II trial, fifty patients who did not respond to other conventional and experimental treatments were administered OV as a monotherapy. An overall positive response was seen in 26% of these patients, with 8 patients experiencing complete response and 5 experiencing partial response. Adverse effects were limited primarily to transient flu-like symptoms. (Senzer *et al.*, 2009). Several other clinical trials in stages I, II, and III are currently being undertaken for a variety of other OV's, including Reovirus, Measles virus, Newcastle disease virus, and VSV (ClinicalTrials.gov, 2012, trial ID NCT01628640; <http://clinicaltrials.gov/ct2/show/NCT01628640>). In terms of safety, results of these trials indicate that even at high doses, OV treatment possesses low toxicity with mild to nonexistent side effects while maintaining robust anti-tumor effects (Breitbach *et al.*, 2010). Despite these encouraging results, the heterogeneous nature of cancer makes the use of monotherapies as complete treatment strategies improbable, and OV's are no exception. Combination with other anticancer treatments will likely be the best approach to exploit the full therapeutic potential of OV's, and will be discussed in later section.

1.3 VSV Virology

VSV is a prototypic enveloped, bullet-shaped, non-segmented, negative-sense, single-stranded RNA virus belonging to the *Rhabdoviridae* family (Lyles and Rupprecht, 2007). Natural hosts include horses, swine, cattle, and several other ungulates along with their insect vectors. VSV produces an acute, non-fatal disease in infected livestock, characterized by fever and blister-like lesions in mucosal tissues (Lichty *et al.*, 2004; Lyles and Rupprecht, 2007). With the exception of agricultural and laboratory workers, there is little pre-existing immunity to VSV in human populations, and VSV infection in humans is generally asymptomatic (Lyles and Rupprecht, 2007).

VSV virions are approximately 180 nm in length and 75 nm in diameter (Whelan, 2008). They contain all five virus-encoded proteins (Lyles & Rupprecht, 2007), as well as a number of host proteins (Moerdyk-Schauwecker *et al.*, 2009). The 11 kb VSV genomic RNA begins with a 3' hydroxyl leader sequence, and contains five mRNAs encoding the nucleocapsid (N) protein, phosphoprotein (P), matrix (M) protein, glycoprotein (G) protein and large polymerase protein (L) (Rodriguez *et al.*, 1999; Whelan, 2008).

Nucleoprotein N forms a complex with the RNA genome to generate the ribonucleoprotein structure (RNP), which protects the virus from host nucleases, and is essential for infection (Whelan, 2008). The G protein enables VSV to infect most mammalian cell types, with a recent study indicating that this occurs through binding ubiquitously expressed low-density lipoprotein (LDL) family receptors (Finkelshtein *et al.*, 2013). Upon attachment, the virus enters the cell through actin- and clathrin-dependent endocytosis. Endosomal acidification facilitates the fusion of the viral envelope with the endosomal membrane, releasing the RNP core into the cytoplasm

where viral mRNA is synthesized (Cureton *et al.*, 2010). Within 20 minutes of virus entry the RNP is uncoated, at which point the viral RNA-dependent RNA polymerase (RdRp, composed of the L and P protein) transcribes a 47-nt leader RNA sequence ending with an untranscribed AAA sequence at its' 3' end, which is used to negatively regulate host transcription in the nucleus (Whelan, 2008; Kurilla *et al.*, 1982). The RdRp then transcribes the viral genome into short mRNA fragments which are capped and polyadenylated poly (A), at which point synthesis of the upstream mRNA is complete (Rodriguez *et al.*, 1999; Ball *et al.*, 1999; Wagner,1996). Each individual mRNA possesses a conserved sequence at its' 5' end recognized by the L protein, which catalyzes a series of GDP-dependent enzymatic reactions that forms the 5' cap (Ogino *et al.*, 2007). The poly(A)-tail is created by a gene junction on the 3' end of each gene with seven U-residues, which causes the polymerase to stutter (Rodriguez *et al.*, 1999). The RdRp proceeds to the next mRNA region to re-initiate transcription by recognizing a 10-nt start sequence following the U-residues at the beginning on each gene (Barr *et al.*, 2002). Through a mechanism that is not fully understood, the polymerase pauses at each intergenic region such that re-initiation of transcription is not 100% efficient. Transcriptions of downstream genes produce a third less mRNA for each subsequent gene as the RdRp progresses (Ball *et al.*, 1999). Each viral gene is transcribed in a sequential and polar order. The N mRNA is produced in the largest amount, followed by P, M, G, and L, respectively.

Host cell ribosomes translate each viral gene. The G protein possesses a signal peptide targeting it to the endoplasmic reticulum (ER) where it is processed and modified.

Amassing of viral proteins, particularly the N protein which is necessary for encapsidation of new genomes, manages transcription vs replication mode of the viral

polymerase. The P protein is also involved in encapsidation, and allows the polymerase to ignore the intergenic pauses and synthesize a full complementary genome (antigenome), which serves as a template for negative-sense genome replication (Patton *et al.*, 1984; Peluso, 1988). Because of sequence differences between the leader and trailer regions, more genomes than antigenomes are created, which generates a second wave of viral transcription and concomitant viral assembly (Finke and Conzelmann, 1997).

Viral proteins are relocated to different cell compartments in order to perform their functions. The N protein is found in the cytosol, complexed with the RNA genome and the P and L polymerase proteins. The G protein is membrane-bound via its synthesis with ER-bound ribosomes, chaperone folding and trimer association at the ER, posttranslational modification at the Golgi and final destination, the host plasma membrane (Bergmann *et al.*, 1981; Doms *et al.*, 1988; Katz and Lodish, 1979). The M protein is produced as a soluble protein found in the cytosol, and is to a lesser extent bound to the membrane (Knipe *et al.*, 1977; Ohno and Ohtake, 1987). Upon viral assembly, the M protein complexes the RNP core to the host plasma membrane containing the G trimers, which promotes the budding of assembled virions (Flood and Lyles, 1999; Odenwald *et al.*, 1986; Harty *et al.*, 2001). VSV infection is quick and efficient, with robust viral replication occurring before the host cell is killed. Lysis of the host cell ends the cycle, and can release up to 100 000 virions per cell, though a large proportion of these are defective particles (Barber, 2005). Maximal virion release is usually achieved within 8-10 hours of infection, slowing down towards the end of the cycle and with induction of apoptosis occurring approximately 16-24 hours post infection (Lyles and Rupprecht, 2007).

1.3.1 VSV pathogenesis: molecular and cellular basis

Host cell defense against VSV replication and infectivity involves the induction of pro-inflammatory cytokines and antiviral genes such as type I interferon (IFN) (Meraz *et al.*, 1996; Muller *et al.*, 1994). IFNs are a family of cytokines that represent the first line of defense against viral infection (Pestka *et al.*, 2004). There are three main subcategories of IFN: Type I (IFN α/β), Type II (IFN γ) and Type III (IFN λ). In type I IFN signaling, ligand binding to IFN receptors, IFN α /beta receptor (IFNAR)1, and IFNAR2 activates the JAK/STAT pathway (De Weerd *et al.*, 2012). Tyrosine kinase 2 and JAK1 activate IFN receptors by phosphorylation and promote STAT1/2 recruitment. A number of IFN-stimulated genes (ISGs) associated with the production of antiviral proteins are upregulated in response to IFN receptor binding (Wang and Fish, 2012). Type I IFN receptor and STAT1 knockdown mice are extremely susceptible to VSV infection (Meraz *et al.*, 1996; Moerdyk-Schauwecker *et al.*, 2013; Muller *et al.*, 1994).

VSV has evolved ways to thwart its detection and elimination by the host, mostly via the M protein. Cytosolic VSV M protein can block tyrosine phosphorylation of STAT3 and interleukin (IL)-6 induced STAT1 and STAT3 activation, thus inhibiting host antiviral and inflammatory responses (Terstegen *et al.*, 2001). The M protein can also suppress IFN β gene expression (Ahmed *et al.*, 2003; Ferran and Luca-Lenard, 1997; Stojdl *et al.*, 2003). This occurs by inhibiting host polymerase function (Ahmed *et al.*, 1998; Lyles, 2000) and by restricting nucleocytoplasmic shuttling of mRNAs (Black *et al.*, 1994; Black and Lyles, 1992; Black *et al.*, 1993; Faria *et al.*, 2005; Ferran and Lucas-Lenard, 1997; Petersen *et al.*, 2000). It appears that residues 51-59 of the M

protein regulate the inhibition of host transcription, and a mutant version of the M protein expressing a methionine to arginine point mutation at residue 51 is unable to block host transcription (Stojdl *et al.*, 2003).

The M protein is also capable of inducing apoptosis, which is widely accepted as a host defense mechanism to restrict viral spread (Kopecky *et al.*, 2001). This pathway is often targeted by viruses as a strategy of host evasion, though VSV's lack of inhibitory mechanisms is very likely due to the short time-frame of its replication cycle (Lyles and Rupprecht, 2007). VSV-induced apoptosis has been demonstrated both intrinsically, via mitochondrial pathways and extrinsically, via death receptor pathways (Cary *et al.*, 2011; Gaddy and Lyles, 2005; Pearce and Lyles, 2009).

1.3.2 VSV as an Oncolytic Virus

VSV bears many of the key features of an ideal OV. As mentioned previously, there is little pre-existing immunity to VSV, and it is generally non-pathogenic in human populations. It can readily infect many cancer cell types, as demonstrated by the high percentage of permissive cells in a panel of 60 cancer cell lines from the National Cancer Institute (NCI60) (Stojdl *et al.*, 2003). Since it has a strictly cytoplasmic replication cycle, there is no chance of host cell genome integration, and it is considered a genetically stable virus. Its basic virology is well-studied, and production of high viral titer stocks is simple and efficient (Barber, 2005; Lichty *et al.*, 2004).

Due to dampened or defective IFN signaling in tumor cells, VSV is able to efficiently replicate in and lyse such cells, while normal cells are spared thanks to an intact

antiviral response. Since the M protein plays such a critical role in VSV's virulence and pathogenicity, mutant forms of VSV, VSV-AV1 and VSV-M Δ 51, were developed to increase VSV's safety profile and therapeutic index (Stojdl *et al.*, 2003). While VSV-AV1 contains a methionine→arginine mutation at residue 51, this residue has been deleted in VSV-M Δ 51, thereby obliterating any chance of reversion. These mutant strains are still able to kill IFN-deficient malignant cells, but unlike WT VSV, they are unable to block host transcription and nucleocytoplasmic RNA transport. As such, in normal, healthy cells, they actually enhance IFN production and the subsequent antiviral response, thus enabling rapid clearance of the virus with minimal damage (Petersen *et al.*, 2000; Stojdl *et al.*, 2003)

In addition to IFN signaling, other abnormal cellular pathways of transformed cells may also play roles in VSV's oncolytic specificity. It has been suggested that double-stranded-RNA-dependent protein kinase (PKR) and defective translational control, as well as cell cycle transition may both contribute to sensitivity to VSV replication and oncolysis (Balachandran and Barber, 2004; Olierie *et al.*, 2008). There is a high level of crosstalk between these pathways, along with the apoptotic and IFN pathways, and they are often mutated in transformed cells. As such, it is likely that they all contribute to sensitivity to VSV oncolysis.

1.3.3 VSV combination treatment strategies

As mentioned above, though VSV has shown promise in preclinical testing, combining the virus with immunomodulators or other anticancer agents appears to be the most efficacious route to take.

One approach involves combining VSV with drugs which restore abnormal pathways of transformed cells, with the goal of sensitizing these cells to VSV-induced apoptosis. Such strategies have been demonstrated in cancer cells known to over-express anti-apoptotic proteins, for example, in B-cell chronic lymphocytic leukemia. These cells over-express the anti-apoptotic B-cell lymphoma 2 protein (Bcl-2), have a defective apoptosis pathway, and are resistant to VSV oncolysis. However, when they are treated with both VSV and Bcl-2 inhibitors, these cells become susceptible to VSV-induced autophagic and apoptotic cell death (Samuel *et al.*, 2010; Tumilasci *et al.*, 2008). Other groups have designed effective treatment strategies using conventional chemotherapeutic agents such as doxorubicin (Schache *et al.*, 2009), as well as multiple OV treatment regimens (Le Boeuf *et al.*, 2010).

Since not all cancer cells exhibit impaired antiviral innate immune responses, combination treatment with immunomodulatory drugs can greatly broaden the range of tumors amenable to VSV therapy. The mammalian target of rapamycin (mTOR) inhibitor rapamycin has been shown to enhance VSV replication and cytotoxicity both in *in vitro* and *in vivo* malignant glioma models by impairing mTOR-dependent type 1 IFN production (Alain *et al.*, 2010). Histone deacetylase inhibitors (HDIs) in combination with VSV, and other OVs, have been shown to synergistically enhance virus replication and cytotoxicity in multiple refractory cancer cell line models and xenografts, with minimal adverse effects on healthy tissues (Nguyen *et al.*, 2008). Though this enhancement is largely due to HDI-mediated suppression of the IFN response, it is likely that other pathways altered by HDI treatment play an important role in contributing to the establishment of a permissive cell environment. For example,

in the case of the VSV-resistant androgen-independent prostate cancer cell line PC3, pretreatment with two different HDIs, MS-275 (Entinostat) and SAHA (Vorinostat), was able to synergistically enhance VSV replication and cell killing. Though HDI treatment was indeed shown to blunt the IFN response, it has been previously shown that PC3, and other resistant cell lines, possess an inherent resistance to VSV infection that is not entirely dependent on IFN signaling (Ahmed *et al.*, 2003; Carey *et al.*, 2008). Thus, it is evident that other factors contribute significantly to VSV resistance in refractory cells, and that HDI treatment is able to overcome these as well

1.4 Histone deacetylase inhibitors

In recent years, the study of epigenetic events in malignancies has brought forth a myriad of mechanisms involved in cancer onset and progression. One such mechanism, histone (de)acetylation, involves histone acetyltransferases (HATs) and histone deacetylases (HDACs), which function to reversibly acetylate/deacetylate both histone and non-histone proteins. There are four classes of HDACs: (I) HDACs 1, 2, 3 and 8; (IIa) HDACs 4, 5, 7 and 9; (IIb) HDACs 6 and 10; (III) sirtuins (NAD-dependent enzymes); and (IV) HDAC11 (Balasubramanian S, *et al.*, 2009). Class I HDACs are ubiquitously expressed and exist as nuclear multi-enzyme complexes acting as transcriptional repressors. Class II HDACs are located in both the cytoplasm and the nucleus, acting as both signal transducers and regulators of cytoplasmic processes (Yang XJ and Seto E., 2008). Class III HDACs are transcriptional and metabolic regulators, and have been implicated in aging and caloric restriction. Strikingly, a frequent occurrence in transformed cells is a high level of HDAC expression with a corresponding hypoacetylation of histones, suggesting an active contribution to tumor

initiation and progression (Weichert, 2009). As such, there has been a focus on HDACs as targets for therapeutic intervention, spurring the development of multiple classes of HDIs. These drugs promote the acetylation of histones and by changes in chromatin structure and transcription factor/cofactor binding, are able to regulate expression of ~2–10% of cellular genes. HDIs are filed into classes according to their chemical structures: hydroxamic acids (Vorinostat/SAHA, Belinostat, ITF2357, Trichostatin A, LAQ824, LBH589), benzamides (Entinostat/MS-275, MBCD0103), and short-chain aliphatic acids (Phenyl Butarate, Valproic Acid). HDIs have exhibited promising anti-tumor activity *in vitro*, in animal models, and in the clinic, though their exact mode of action has not been fully elucidated and appears to be cell type, compound, and context-dependent. A number of mechanisms have been suggested, including cell cycle arrest, differentiation, up-regulation of tumor suppressors, down-regulation of mitogenic factors, inhibition of DNA repair, oxidative stress, anti-angiogenesis, induction of autophagy, and induction of apoptosis (Balasubramanian *et al.*, 2009; Bolden *et al.*, 2006; Glaser *et al.*, 2007; Rosato and Grant, 2005; Xu *et al.*, 2007; New *et al.*, 2012). The wide ranging effects of HDIs is directly related to the ubiquity of acetylation: they not only affect transcription, but also protein interactions, localization, stability, and DNA binding (Buchwald *et al.*, 2009). Several HDIs are currently in clinical trials, and two, Romidepsin, which is selective for class I enzymes, and Vorinostat, which inhibits all zinc dependent HDACs of classes I, IIa, IIb, and IV, have been FDA approved for treatment of cutaneous T-cell lymphoma (CTCL) (Ververis *et al.*, 2013). Though HDIs have been proven effective against certain hematological malignancies, their effectiveness against solid tumors has not been met with as much success. As such, employing them in combination with other agents, particularly OV, has garnered interest.

1.4.1 Mechanisms of HDI-mediated enhancement of OV therapy

A variety of HDIs and OVs have been combined and demonstrated effectiveness in *in vitro* and *in vivo* studies. As mentioned above, vorinostat and entinostat have been combined with VSV in colon, breast, prostate, ovarian, melanoma, and lung cancer models to enhance virus replication, synergistically induce cell death, reduce tumor growth and cause vascular shutdown (Nguyen *et al.*, 2008). Another strategy involves using HDIs to alter expression of viral receptors present on cancer cells. Romidepsin, entinostat, and other HDIs have been shown to upregulate expression of cellular coxsackie and adenovirus receptor (CAR), which in tumors refractory to adenoviral infection, is often missing or greatly underexpressed. This combination enhanced adenoviral infection in multiple cancer cell lines, with minimal effect in normal tissues (Kitazano *et al.*, 2001; Kitazano *et al.*, 2002; Goldsmith *et al.*, 2003). The activation of other growth/immunomodulatory pathways by HDIs, such as nuclear factor kappa-light-chain enhancer of activated B cells (NF- κ B) has also been exploited as a means to improve OV therapy. For example, Katsura *et al.* studied the effectiveness of combining an oncolytic HSV strain with Trichostatin A (TSA) in oral squamous carcinoma cells (Katsura *et al.*, 2009). They found that pretreatment with TSA increased HSV replication through a mechanism that was dependent on enhanced nuclear translocation and acetylation of the NF- κ B transcription factor subunit RelA/p65, indicating that HDI-mediated stimulation of the NF- κ B pathway improves HSV replication and oncolytic activity.

Another pathway that could be of great interest to the mechanistics of HDI and OV

synergy, but is only beginning to be explored, is autophagy. HDIs have been shown to induce autophagy in cancer cells, though it can act as either a pro-survival or pro-death mechanism (Carew *et al.*, 2008; Gammoh *et al.*, 2012). However, in the context of combination therapy with certain OV, autophagy may contribute positively to virus replication, spread, and subsequent lysis of the tumor tissue. Indeed, several groups have demonstrated increased viral replication, yield, and spread, enhanced antitumor effect and significantly improved survival rates of mice bearing xenografts when autophagy-inducing agents are administered alongside OV such as adenovirus (Alonso *et al.*, 2008; Yokoyama *et al.*, 2008), myxoma virus (Lun *et al.*, 2007; Stanford *et al.*, 2008; Lun *et al.*, 2010), HSV (Fu *et al.*, 2011), and vaccinia virus (Lun *et al.*, 2009).

1.5 NF- κ B Signaling

The NF- κ B pathway is a central mediator of stress and immune responses. In the canonical pathway, the NF- κ B transcription factor subunits (RelA/p65 and p50, which exist as hetero or homodimers) are held in a latent state by the inhibitor of κ B (I κ B) proteins. This family of proteins contains multiple ankyrin repeat domains, which mask the nuclear localization signals (NLS) of the transcription factor subunits, thus sequestering them in the cytoplasm. A variety of signals, such as stress, cytokines, and pathogens, activate the inhibitor of κ B kinase (IKK) complex, composed of a trimer of two catalytic proteins, IKK α and IKK β along with the regulatory NF- κ B essential modulator (NEMO) (Gilmore, 2006). This leads to the IKK-mediated phosphorylation of two serine residues in the regulatory domain of I κ B, targeting it for ubiquitination and proteasomal degradation. The unmasked NF- κ B transcription factor subunits are then free to translocate to the nucleus and activate transcription of target genes

containing κB binding sites in their promoter regions, leading to a variety of physiological responses including but not limited to inflammation, immune response, cell survival, or cell death. Specificity of gene expression is dependent upon several factors, such as the combination of subunits in the transcription factor dimer, and post-translational modifications, such as phosphorylation and acetylation, of said subunits (Perkins, 2007). NF- κB also activates expression of its own repressor, I κB . The newly synthesized I κB re-associates and thus re-inhibits NF- κB , shuttling it out of the nucleus. This generates an auto feedback loop, resulting in oscillating levels of NF- κB activity (Nelson *et al.*, 2004).

1.5.1 Role of NF- κB in Viral Infections

It is well established that activation of NF- κB along with interferon regulatory factor (IRF) is an essential, immediate early step in the cellular innate immune response to viral infection. Briefly, the generally accepted consensus is that in most cell types, RNA viruses are recognized by the retinoic acid-inducible I (RIG-I)-like receptor (RLR) family of pathogen sensors, which triggers activation of three classes of transcription factors: IRFs-3 and 7, NF- κB and activating Transcription Factor 2 (ATF-2/c-Jun) (Akira *et al.*, 2006; Yoneyama and Fujita, 2009; Hiscott, 2007), which then bind sites in the IFN β enhancer region to create the “enhanceosome”. This complex recruits other transcription factors and chromatin-modifiers to commence transcription of IFN β , and the subsequent type I IFN antiviral innate immune response (Munshi *et al.*, 1999; Maniatis *et al.*, 1998; Thanos and Maniatis, 1995). As a result of its early necessity, NF- κB represents an attractive option for viral interference. Many viruses are able to inhibit innate immune responses via viral proteins which specifically target particular

components of the pathway, however many others actually subvert NF- κ B signaling to support their own replication. This is due to the fact that despite its requirement for IFN β induction, NF- κ B also regulates a number of other pathways whose manipulation is often beneficial to the viral life cycle, including apoptosis and proliferation (Hiscott *et al.*, 2006).

1.5.2 Cross-talk between NF- κ B and autophagy

NF- κ B signaling mediates a large number of pathways, and in recent years a number of studies have emerged indicating a high level of crosstalk between NF- κ B and autophagic signaling. For example, the NF- κ B transcription factor subunit RelA/p65 appears to be essential for transcription of key autophagy related genes (Atgs), such as Beclin-1 (Copetti *et al.*, 2009), while the upstream IKK complex is required for autophagy induction by multiple stimuli (Criollo *et al.*, 2010). Similarly, NF- κ B signaling is blocked in mouse embryonic fibroblasts (MEFs) and cancer cells depleted of essential Atgs, including Atg5, Atg7, and Beclin-1, underlining a mutual essentiality between these two pathways (Criollo *et al.*, 2012).

1.6 Autophagy

Autophagy is an essential, homeostatic process by which cells sequester and degrade their own components for degradation using the lysosomal machinery. It is a mechanism of self-digestion, and plays a role in survival, cellular restructuring, and recycling of organelles (Levine and Klionsky, 2004; Mizushima, 2007). The study of autophagy has grown considerably in recent years, with particular foci on its contribution to immune regulation, viral infection, and disease development.

A number of stimuli can cause induction of autophagy, including hypoxia, dysfunctional organelles, starvation, and superfluous/foreign cytosolic components. Briefly, targeted cytosolic components are sequestered into a small vesicular sac (the phagophore), which elongates into a large double-membrane vesicle known as the autophagosome. The endosome fuses with the outer membrane of the autophagosome, maturing into the amphisome. The amphisomes then fuse with the lysosome to create autophagolysosomes, wherein the interior components are degraded (Mizushima *et al.*, 2010). Many cellular factors contribute to this process, among them a group known as the autophagy-related genes (Atgs) first identified in yeast (Levine and Klionsky, 2004). In mammalian cells, Atgs promote specific cargo selection, vesicle elongation, and membrane fusion, and are essential for autophagy to occur.

1.6.1 Autophagy & Viral Infections

Autophagy is emerging as an important mechanism by which intracellular pathogens can be specifically targeted for degradation, and as a trigger for launching innate immune responses (Levine *et al.*, 2011). Conversely, for other viruses, it can actually support viral replication and spread (Orvedahl and Levine, 2009).

Several groups have demonstrated a protective role for autophagy in the host antiviral response. For example, viral nucleic acids and protein products generated by degradation of viral particles are sensed as antigens which prompt innate and adaptive immune responses (Levine and Deretic, 2007; Lee *et al.*, 2007; Gannage and Munz, 2009). However, in other instances autophagy can positively regulate virus replication. Such appears to be the case with VSV, whose replication has been shown to be dependent on autophagy (Jounai *et al.*, 2007). Upon infection, the

Atg5-Atg12 conjugate, a key mediator of autophagy, inhibits type I IFN production by directly blocking the crucial innate antiviral proteins RIG-I and IFN β promoter stimulator 1 (IPS-1) through their caspase recruitment domains (CARDs). The autophagic machinery itself can also be used as a physical scaffold to support replication, as is the case with poliovirus and coxsackievirus (Jackson *et al.*, 2005; Wong *et al.*, 2008).

1.6.2 Autophagy & Cancer

Similarly to its role in viral infections, autophagy can also play dual, context-specific roles in cancer to either promote or block tumorigenesis (Shen and Codogno, 2011; White, 2012).

As a pro-survival mechanism, it is evident why cancer cells may activate autophagy as a result of the inhospitable tumor microenvironment. Stressful conditions arising from depleted nutrient levels and hypoxia trigger autophagy, maintaining mitochondrial metabolism and allowing the tumor to grow (Guo *et al.*, 2011; Degenhardt *et al.*, 2006). On the other hand, autophagy can also inhibit tumorigenesis via degradation of oncogenic proteins and dysfunctional organelles (White, 2012). Depletion of the autophagy gene Beclin-1 is associated with a number of human cancers (Liang *et al.*, 1999; Aita *et al.*, 1999), and double-knockout of this gene in mice increases spontaneous malignancies (Qu *et al.*, 2003; Yue *et al.*, 2003). Multiple ATG genes, such as ATG2B, ATG5, ATG9B, and ATG12 are mutated in gastric and colorectal cancers (Kang *et al.*, 2009). Additionally, autophagy can contribute cancer cell death, either via its own unique, though highly debated and controversial, mechanism of

programmed cell death (Shen and Codogno, 2011; Shen *et al.*, 2012) or via its extensive crosstalk with the apoptotic pathway (Su *et al.*, 2013).

References

- Ahmed, M. and Lyles, D.S. (1998). Effect of vesicular stomatitis virus matrix protein on transcription directed by host RNA polymerases I, II, and III. *J Virol.* 72:8413-8419.
- Ahmed, M., McKenzie, M.O., Puckett, S., Hojnacki, M., Poliquin, L., Lyles, D. S. (2003). Ability of the matrix protein of vesicular stomatitis virus to suppress beta interferon gene expression is genetically correlated with the inhibition of host RNA and protein synthesis. *J Virol*, 77:4646-4657.
- Aita, V.M., Liang, X.H., Murty, V.V., Pincus, D.L., Yu, W., Cayanis, E. et al. (1999). Cloning and genomic organization of beclin 1, a candidate tumor suppressor gene on chromosome 17q21. *Genomics.* 59:59-65
- Akira, S., Uematsu, S., Takeuchi, O. (2006). Pathogen recognition and innate immunity. *Cell.* 124:783–801.
- Alain, T., Lun, X., Martineau, Y., Sean, P., Pulendran, B., Petroulakis, E., Zemp, F.G., Lemay, C.G., Roy, D., Bell, J.C., Thomas, G., Kozma, S.C., Forsyth, P.A., Costa-Mattioli, M., Sonenberg, N. (2010). Vesicular stomatitis virus oncolysis is potentiated by impairing mTORC1-dependent type I IFN production. *Proc Natl Acad Sci U S A.* 107:1576-81.
- Alonso, M.M., Jiang, H., Yokoyama, T., et al. (2008). Delta-24-RGD in combination with RAD001 induces enhanced anti-glioma effect via autophagic cell death. *Mol Ther.* 16:487-93.
- Balachandran, S., and Barber, G.N. (2004). Defective translational control facilitates vesicular stomatitis virus oncolysis. *Cancer Cell.* 5:51-65.
- Balasubramanian, S., Verner, E., Buggy, J.J. (2009) Isoform-specific histone deacetylase inhibitors: the next step? *Cancer Lett.* 280:211–21.
- Ball, L.A., Pringle, C.R., Flanagan, B., Perepelitsa, V.P., Wertz, G.W. (1999). Phenotypic consequences of rearranging the P, M, and G genes of vesicular stomatitis virus. *J Virol*, 73:4705-4712.
- Barber, G.N. (2005). VSV-tumor selective replication and protein translation. *Oncogene.* 24:7710-9.
- Barr, J.N., Whelan, S.P., Wertz, G.W. (2002). Transcriptional control of the RNA-dependent RNA polymerase of vesicular stomatitis virus. *Biochim Biophys Acta.* 1577:337-353.

Bergmann, J.E., Tokuyasu, K.T., Singer, S.J. (1981). Passage of an integral membrane protein, the vesicular stomatitis virus glycoprotein, through the Golgi apparatus en route to the plasma membrane. *Proc Natl Acad Sci U S A*. 78:1746-50.

Black, B.L., Brewer, G., Lyles, D.S. (1994). Effect of vesicular stomatitis virus matrix protein on host-directed translation in vivo. *J Virol*, 68:555-560.

Black, B.L. and Lyles, D.S. (1992). Vesicular stomatitis virus matrix protein inhibits host cell-directed transcription of target genes in vivo. *J Virol*, 66:4058-4064.

Black, B.L., Rhodes, R.B., McKenzie, M., Lyles, D.S. (1993). The role of vesicular stomatitis virus matrix protein in inhibition of host-directed gene expression is genetically separable from its function in virus assembly. *J Virol*. 67:4814-4821.

Bluming, A.Z., and Ziegler, J.L. (1971). Regression of Burkitt's lymphoma in association with measles infection. *Lancet*. 2:105-106.

Bolden, J.E., Peart, M.J., Johnstone, R.W. (2006). Anticancer activities of histone deacetylase inhibitors. *Nat Rev Drug Discov*. 5:769–84.

Borley, N., Feneley, M.R. (2009). Prostate cancer: Diagnosis and staging. *Asian J. Androl*. 11:74–80.

Breitbach, C.J., Reid, T., Burke, J., Bell, J.C., Kim, D.H. (2010). Navigating the clinical development landscape for oncolytic viruses and other cancer therapeutics: no shortcuts on the road to approval. *Cytokine Growth Factor Rev*. 21:85-9.

Bubendorf, L., Schöpfer, A., Wagner, U., et al. (2000). Metastatic patterns of prostate cancer: an autopsy study of 1,589 patients. *Human Pathology*. 31:578–583.

Buchwald, M., Kramer, O.H., Heinzel, T. HDACi-targets beyond chromatin. *Cancer Lett*. 280:160–167.

Cairns, R.A., I.S. Harris, and T.W. Mak. (2011). Regulation of cancer cell metabolism. *Nat Rev Cancer*. 11:85-95.

Carew, J.S., Giles, F.J., Nawrocki, S.T. (2008) Histone deacetylase inhibitors: mechanisms of cell death and promise in combination cancer therapy. *Cancer Lett*. 269:7-17.

Carey, B., Ahmed, M., Puckett, S., Lyles, D.S. (2008) Early steps of the virus replication cycle are inhibited in prostate cancer cells resistant to oncolytic vesicular stomatitis virus. *J Virol*. 82:12104-12115.

Cary, Z.D., Willingham, M.C., Lyles, D.S. (2011). Oncolytic vesicular stomatitis virus induces apoptosis in U87 glioblastoma cells by a type II death receptor mechanism and induces cell death and tumor clearance in vivo. *J Virol*. 85:5708-5717.

- Chattopadhyay, S., Marques, J.T., Yamashita, M., Peters, K.L., Smith, K., Desai, A., Williams, B.R.G., Sen, G. (2010). Viral apoptosis is induced by IRF-3 mediated activation of Bax. *EMBO J.* 29:1762-1773.
- Christian, S.L., Collier, T.W., Zu, D., Licursi, M., Hough, C.M., Hirasawa, K. (2009). Activated Ras/MEK inhibits the antiviral response of alpha interferon by reducing STAT2 levels. *J Virol.* 83:6717-6726.
- Constantinescu, S.N., Girardot, M., Pecquet, C. (2008). Mining for JAK-STAT mutations in cancer. *Trends Biochem Sci.* 33:122-31.
- Copetti, T., Demarchi, F., Schneider, C. (2009). p65/RelA modulates BECN1 transcription and autophagy. *Mol Cell Biol.* 29:2594-2608.
- Criollo, A., Senovilla, L., Authier, H., Maiuri, M.C., et al. (2010). The IKK complex contributes to the induction of autophagy. *EMBO J.* 29:619-631.
- Criollo, A., Chereau, F., Malik, S.A., Niso-Santano, M., Marino, G., Galluzzi, L., Maiuri, M.C., Baud, V., Kroemer, G. (2012). Autophagy is required for the activation of NF- κ B. *Cell Cycle.* 11:194-199.
- Critchley-Thorne, R.J., Simons, D.L., Yan, N., Miyahira, A.K., Dirbas, F.M., Johnson, D.L., Swetter, S.M., Carlson, R.W., Fisher, G.A., Koong, A., Holmes, S., & Lee, P.P. (2009). Impaired interferon signaling is a common immune defect in human cancer. *Proc Natl Acad Sci U S A.* 106:9010-9015.
- Cureton, D.K., Massol, R.H., Whelan, S.P., Kirchhausen, T. (2010). The length of vesicular stomatitis virus particles dictates a need for actin assembly during clathrin-dependent endocytosis. *PLoS Pathog.* 6(9), e1001127.
- Degenhardt, K., Mathew, R., Beaudoin, B., Bray, K., Anderson, D., Chen, G., Mukherjee, C., Shi, Y., Gelinas, C., Fan, Y., Nelson, D.A., Jin, S., White, E. (2006). Autophagy promotes tumor cell survival and restricts necrosis, inflammation, and tumorigenesis. *Cancer Cell.* 10:51-64.
- De Weerd, N.A., and Nguyen, T. (2012). The interferons and their receptors-distribution and regulation. *Immunol Cell Biol.* 90:483-491.
- Doms, R.W., Ruusala, A., Machamer C., Helenius, J., Helenius, A., Rose, J.K. (1988.) Differential effects of mutations in three domains on folding, quaternary structure, and intracellular transport of vesicular stomatitis virus G protein. *J Cell Biol.* 107:89-99
- Downward, J. (2003). Targeting RAS signaling pathways in cancer therapy. *Nat Rev Cancer.* 3:11-22.
- Drake, C.G. (2010). Prostate cancer as a model for tumour immunotherapy. *Nat Rev Immunol.* 10:580-93.
- Elmore, S. (2007). Apoptosis: a review of programmed cell death. *Toxicol Pathol.* 35:495-516.

Faria, P.A., Chakraborty, P., Levay, A., Barber, G.N., Ezelle, H.J., Enninga, J., Arana, C., van Deursen, J., Fontoura, B.M. (2005). VSV disrupts the Rae1/mrnp41 mRNA nuclear export pathway. *Mol Cell*. 17:93-102.

Ferran, M.C. and Lucas-Lenard, J.M. (1997). The vesicular stomatitis virus matrix protein inhibits transcription from the human beta interferon promoter. *J Virol*. 71:371-377.

Finke, S., and Conzelmann, K.K. (1997). Ambisense gene expression from recombinant rabies virus: random packaging of positive- and negative-strand ribonucleoprotein complexes into rabies virions. *J Virol*. 71:7281-8.

Finkelshtein, D., Werman, A., Novick, D., Barak, S., Rubinstein, M. (2013) LDL receptor and its family members serve as the cellular receptors for vesicular stomatitis virus. *Proc Natl Acad Sci U S A*. 110:7306-7311.

Flood, E.A., and Lyles, D.S. (1999). Assembly of nucleocapsids with cytosolic and membrane-derived matrix proteins of vesicular stomatitis virus. *Virology*. 261:295-308.

Fu, X., Tao, L., Rivera, A., et al. (2011). Rapamycin enhances the activity of oncolytic herpes simplex virus against tumor cells that are resistant to virus replication. *Int J Cancer*. 129:1503-10

Gaddy, D.F., and Lyles, D.S. (2005). Vesicular stomatitis viruses expressing wild-type or mutant M proteins activate apoptosis through distinct pathways. *J Virol*. 79:4170- 9.

Gammoh, N., Lam, D., Puente, C., et al. (2012). Role of autophagy in histone deacetylase inhibitor-induced apoptotic and nonapoptotic cell death. *Proc Natl Acad Sci U S A*. 109:6561-6565

Gannage, M. and Munz, C. (2009). Autophagy in MHC class II presentation of endogenous antigens. *Curr Top Microbiol Immunol*. 335:123-140.

Garber, K. (2006). China approves world's first oncolytic virus therapy for cancer treatment. *J Natl Cancer Inst*. 98:298-300.

Gilmore, T.D. (2006). Introduction to NF- κ B: players, pathways, perspectives. *Oncogene*. 25:6680–6684.

Glaser, K.B. (2007). HDAC inhibitors: clinical update and mechanism-based potential. *Biochem Pharmacol*. 74:659–71.

Goldsmith, M.E., Kitazono, M., Fok, P., Aikou, T., Bates, S., Fojo, T. (2003). The histone deacetylase inhibitor FK228 preferentially enhances adenovirus transgene expression in malignant cells. *Clin Cancer Res*. 9:5394–5401.

Guo, J.Y., Chen, H.Y., Mathew, R., Fan, J., Strohecker, A.M., Karsli-Uzunbas, G., Kamphorst, J.J., Chen, G., Lemons, J.M., Karantza, V., Collier, H.A., Dipaola, R.S.,

- Gelinas, C., Rabinowitz, J.D., White, E. (2011). Activated Ras requires autophagy to maintain oxidative metabolism and tumorigenesis. *Genes Dev.* 25:460-470.
- Hanahan, D., and Weinberg, R.A. (2000). The hallmarks of cancer. *Cell.* 100:57-70.
- Harty, R.N., Brown, M.E., McGettigan, J.P., Wang, G., Jayakar, H.R., Huibregtse, J.M., Whitt, M.A., Schnell, M.J. (2001). Rhabdoviruses and the cellular ubiquitin-proteasome system: a budding interaction. *J Virol.* 75:10623-9.
- Hiscott, J, Nguyen, T.L., Arguello, M., Nakhaei, P., Paz, S. (2006). Manipulation of the NF- κ B pathway and the innate immune response by viruses. *Oncogene.* 25:6844-6867.
- Hiscott, J. (2007). Convergence of the NF-kappaB and IRF pathways in the regulation of the innate antiviral response. *Cytokine Growth Factor Rev.* 18:483–490.
- Hollstein, M., Sidransky, D., Vogelstein, B., Harris, C.C. (1991). p53 mutations in human cancers. *Science.* 253:49-53.
- Jackson, W.T., Giddings, T.H., Jr., Taylor, M.P., Mulinyawe, S., Rabinovitch, M., Kopito, R.R., Kirkegaard, K. (2005). Subversion of cellular autophagosomal machinery by RNA viruses. *PLoS Biol.* 3:e156.
- Jounai, N., Takeshita, M., Kobiyama, K., Sawana, S., et al. (2007). The Atg5-Atg12 conjugate associates with innate antiviral immune responses. *Proc Natl Acad Sci U S A.* 104:14050-14055.
- Kang, M.R., Kim, M.S., Oh, J.E., Kim, Y.R., Song, S.Y., et al. (2009). Frameshift mutations of autophagy-related genes ATG2B, ATG5, ATG9B and ATG12 in gastric and colorectal cancers with microsatellite instability. *Journal of Pathology.* 217:702-706.
- Katsura, T., Iwai, S., Ota, Y., Shimizu, H., Ikuta, K., Yura, Y. (2009). The effects of trichostatin A on the oncolytic ability of herpes simplex virus for oral squamous carcinoma cells. *Canc Gene Ther.* 16:237-245.
- Katz, F.N., and Lodish, H.F. (1979). Transmembrane biogenesis of the vesicular stomatitis virus glycoprotein. *J Cell Biol.* 80:416-26.
- Kelly, E., and Russell, S.J. (2007). History of oncolytic viruses: genesis to genetic engineering. *Mol Ther.* 15:651-9.
- Kitazono, M., Goldsmith, M.E., Aikou, T., Bates, S., Fojo, T. (2001). Enhanced adenovirus transgene expression in malignant cells treated with the histone deacetylase inhibitor FR901228. *Cancer Res.* 61:6328–30.
- Kitazono, M., Rao, V.K., Robey, R., Aikou, T., Bates, S., Fojo, T., et al. (2002). Histone deacetylase inhibitor FR901228 enhances adenovirus infection of hematopoietic cells. *Blood.* 99:2248–2251.

- Knipe, D.M., Baltimore, D., Lodish, H.F. (1977). Separate pathways of maturation of the major structural proteins of vesicular stomatitis virus. *J Virol.* 21:1128-39
- Kopecky, S.A., Willingham, M.C., Lyles, D.S. (2001). Matrix protein and another viral component contribute to induction of apoptosis in cells infected with vesicular stomatitis virus. *J Virol.* 75:12169-81.
- Kurilla, M.G., Piwnica-Worms, H., Keene, J.D. (1982). Rapid and transient localization of the leader RNA of vesicular stomatitis virus in the nuclei of infected cells. *Proc Natl Acad Sci U S A*, 79:5240-5244.
- Le Boeuf, F., Diallo, J.S., McCart, J.F., Thorne, S., Falls, T., Stanford, M., Kanji, F., Auer, R., Brown, C.W., Lichty, B.D., Parato, K., Atkins, H., Kirn, D., Bell, J.C. (2010). Synergistic interaction between oncolytic viruses augments tumor killing. *Mol Ther.* 18:888-95.
- Lee, H.K., Lund, J.M., Ramanathan, B., Mizushima, N., Iwasaki, A. (2007). Autophagy-dependent viral recognition by plasmacytoid dendritic cells. *Science.* 315:1398-1401.
- Levine, B., and Klionsky, D.J. (2004). Development by self-digestion: molecular mechanisms and biological functions of autophagy. *Dev Cell.* 6:463-477.
- Levine, B. and Deretic, V. (2007). Unveiling the roles of autophagy in innate and adaptive immunity. *Nat Rev Immunol.* 7:767-777.
- Levine, B., Mizushima, N., Virgin, H.W. (2011). Autophagy in immunity and inflammation. *Nature.* 469:323-335.
- Liang, X.H., Jackson, S., Seaman, M., Brown, K., Kempkes, B., Hibshoosh, H. et al. (1999). Induction of autophagy and inhibition of tumorigenesis by beclin 1. *Nature.* 402:672-676
- Lichty, B.D., Power, A.T., Stojdl, D.F., and Bell, J.C. (2004). Vesicular stomatitis virus: re-inventing the bullet. *Trends Mol Med.* 10:210-6.
- Lun, X.Q., Zhou, H., Alain, T., et al. (2007). Targeting human medulloblastoma: oncolytic virotherapy with myxoma virus is enhanced by rapamycin. *Cancer Res.* 67:8818-8827.
- Lun, X.Q., Jang, J.H., Tang, N., et al. (2009). Efficacy of systemically administered oncolytic vaccinia virotherapy for malignant gliomas is enhanced by combination therapy with rapamycin or cyclophosphamide. *Clin Cancer Res.* 15:2777-2788
- Lun, X.Q., Alain, T., Zemp, F.J., et al. (2010). Myxoma virus virotherapy for glioma in immunocompetent animal models: optimizing administration routes and synergy with rapamycin. *Cancer Res.* 70:598-608.
- Lyles, D.S. (2000). Cytopathogenesis and inhibition of host gene expression by RNA viruses. *Microbiol Mol Biol Rev.* 64:709-724.

- Lyles, D.S., and Rupprecht, C.E. (2007). Rhabdoviridae. Wolters Kluwer Health/Lippincott Williams & Wilkins, Philadelphia.
- Maniatis T, Falvo JV, Kim TH, Kim TK, Lin CH, et al. (1998). Structure and function of the interferon-beta enhanceosome. *Cold Spring Harb Symp Quant Biol.* 63:609–620.
- Mapara, M.Y., and Sykes, M. (2004). Tolerance and cancer: mechanisms of tumor evasion and strategies for breaking tolerance. *J Clin Oncol.* 22:1136-1151.
- Meraz, M.A., White, J.M., Sheehan, K.C., Bach, E.A., Rodig, S.J., Dighe, A.S., Kaplan, D.H., Riley, J.K., Greenlund, A.C., Campbell, D., Carver-Moore, K., DuBois, R.N., Clark, R., Aguet, M., Schreiber, R.D. (1996). Targeted disruption of the Stat1 gene in mice reveals unexpected physiologic specificity in the JAK-STAT signaling pathway. *Cell.* 84:431-42.
- Mizushima, N. (2007). Autophagy: process and function. *Genes Dev.* 21:2861-2873.
- Mizushima, N., Yoshimori, T., Levine, B. (2010). Methods in mammalian autophagy research. *Cell.* 140:313-326.
- Muller, U., Steinhoff, U., Reis, L.F., Hemmi, S., Pavlovic, J, Zinkernagel, R.M., Aguet, M. (1994). Functional role of type I and type II interferons in antiviral defense. *Science.* 264:1918-21.
- Munshi N, Yie Y, Merika M, Senger K, Lomvardas S, et al. (1999) The IFN-beta enhancer: a paradigm for understanding activation and repression of inducible gene expression. *Cold Spring Harb Symp Quant Biol.* 64:149–159.
- Moerdyk-Schauwecker, M., Hwang, S.I., Grdzlishvili, V.Z. (2009). Analysis of virion associated host proteins in vesicular stomatitis virus using a proteomics approach. *J Virol.* 6:166.
- Moerdyk-Schauwecker, M., Shah, N.R., Murphy, A.M., Hastie, E., Mukherjee, P., Grdzlishvili, V.Z. (2013). Resistance of pancreatic cancer cells to oncolytic vesicular stomatitis virus: role of type I interferon signaling. *Virology.* 436:221-234.
- New, M., Olzscha, H., La Thangue, N.B. HDAC inhibitor-based therapies: can we interpret the code? *Mol Oncol.* 6:637-656.
- Nguyen, T.L., Abdelbary, H., Arguello, M., Breitbach, C., Leveille, S., Diallo, J.S., Yasmeen, A., Bismar, T., Kirn, D., Snoultten, V., Vanderhyden, B., Werier, J., Atkins, H., Vaha-Koskela, M., Stojdl, D., Bell, J.C., Hiscott, J. (2008) Chemical targeting of the innate antiviral response by histone deacetylase inhibitors renders refractory cancers sensitive to viral oncolysis. *Proc Natl Acad Sci U S A.* 105:14981- 14986.
- Nelson DE, Ihekweba AE, Elliott M, Johnson JR, Gibney CA, Foreman BE, Nelson G, See V, Horton CA, Spiller DG, Edwards SW, McDowell HP, Unitt JF, Sullivan E,

- Grimley R, Benson N, Broomhead D, Kell DB, White MR (2004). "Oscillations in NF- κ B signaling control the dynamics of gene expression". *Science*. 306:704–708.
- Odenwald, W.F., Arnheiter, H., Dubois-Dalcq, M., Lazzarini, R.A. (1986). Stereo images of vesicular stomatitis virus assembly. *J Virol*. 57:922-32.
- Ogino, T., and Banerjee, A.K. (2007). Unconventional mechanism of mRNA capping by the RNA-dependent RNA polymerase of vesicular stomatitis virus. *Mol Cell*. 25:85-97.
- Ohno, S., and Ohtake, N. (1987). Immunocytochemical study of the intracellular localization of M protein of vesicular stomatitis virus. *Histochem J*. 19:297-306
- Oliere, S., Arguello, M., Mesplede T., Tumilasci, V., Nakhaei, P., Stojdl, D., Sonenberg, N., Bell, J., Hiscott, J. (2008) Vesicular stomatitis virus oncolysis of T lymphocytes requires cell cycle entry and translation initiation. *J Virol*. 82:5735-5749.
- Orvedahl, A. and Levine, B. (2009). Autophagy in mammalian antiviral immunity. *Curr Top Microbiol Immunol*. 335:267-285.
- Ouyang, L., Shi, Z., Zhao, S., Wang, F.T., Zhou, T.T., Liu, B., & Bao, J.K. (2012). Programmed cell death pathways in cancer: a review of apoptosis, autophagy and programmed necrosis. *Cell Prolif*. 45:487-498.
- Parato, K.A., Senger, D., Forsyth, P.A., & Bell, J.C. (2005). Recent progress in the battle between oncolytic viruses and tumors. *Nat Rev Cancer*. 5:965-976.
- Pasquinucci, G. (1971). Possible effect of measles on leukaemia. *Lancet*. 1:136.
- Pattingre, S., and Levine, B. (2006). Bcl-2 inhibition of autophagy: a new route to cancer? *Cancer Res*. 66:2885-2888.
- Patton, J.T., Davis, N.L., Wertz, G.W. (1984). N protein alone satisfies the requirement for protein synthesis during RNA replication of vesicular stomatitis virus. *J Virol*. 49:303-9.
- Pearce, A.F., and Lyles, D.S. (2009). Vesicular stomatitis virus induces apoptosis primarily through Bak rather than Bax by inactivating Mcl-1 and Bcl-XL. *J Virol*. 83:9102-12.
- Peluso, R.W. (1988). Kinetic, quantitative, and functional analysis of multiple forms of the vesicular stomatitis virus nucleocapsid protein in infected cells. *J Virol*. 62:2799-807.
- Perkins, N.D. (2007). Integrating cell-signalling pathways with NF-kappaB and IKK function. *Nat Rev Mol Cell Biol*. 8:49-62.
- Pestka, S., Krause, C.D., Walter, M.R. (2004). Interferons, interferon-like cytokines, and their receptors. *Immunol Rev*. 202:8-32

- Petersen, J.M., Her, L.S., Varvel, V., Lund, E., Dahlberg, J.E. (2000). The matrix protein of vesicular stomatitis virus inhibits nucleocytoplasmic transport when it is in the nucleus and associated with nuclear pore complexes. *Mol Cell Biol*, 20:8590-8601.
- Qu, X., Yu, J., Bhagat, G., Furuya, N., Hibshoosh, H., Troxel, A., Rosen, J., Eskelinen, E.L., Mizushima, N., Ohsumi, Y., Cattoretti, G., Levine, B. (2003). Promotion of tumorigenesis by heterozygous disruption of the beclin 1 autophagy gene. *J Clin Invest.*, 112:1809-1820.
- Rodriguez, L.L., Nichol, S.T., Webster, R.G., Granoff, A. (1999). *Encyclopedia of Virology* (2nd ed.). London: Academic Press.
- Rosato, R.R. and Grant, S. (2005). Histone deacetylase inhibitors: insights into mechanisms of lethality. *Expert Opin Ther Targets*. 9:809–824
- Samuel, S., Tumilasci, V., Olier, S., Nguyen, T.L., Shamy, A., Bell, J., Hiscott, J. (2010). VSV oncolysis in combination with the BCL-2 inhibitor obatoclax overcomes apoptosis resistance in chronic lymphocytic leukemia. *Mol Ther*. 18:2094-103.
- Schache P, Gurlevik E, Struver N, et al. (2009). VSV virotherapy improves chemotherapy by triggering apoptosis due to proteasomal degradation of Mcl-1. *Gene Ther*. 16:849-861.
- Senzer, N.N., Kaufman, H.L., Amatruda, T., Nemunaitis, M., Reid, T., Daniels, G., Gonzalez, R., Glaspy, J., Whitman, E., Harrington, K., Goldsweig, H., Marshall, T., Love, C., Coffin, R., Nemunaitis, J.J. (2009). Phase II clinical trial of a granulocyte-macrophage colony-stimulating factor-encoding, second-generation oncolytic herpesvirus in patients with unresectable metastatic melanoma. *J Clin Oncol*. 27:5763-71.
- Shen, M.M and Abate-Shen, C. (2010). Molecular genetics of prostate cancer: new prospects for old challenges. *Genes Dev*. 24:1967-2000.
- Shen, H.M. and Codogno, P. (2011). Autophagic cell death: Loch Ness monster or endangered species? *Autophagy*. 7:457-465.
- Shen, S., Kepp, O., Kroemer, G. (2012). The end of autophagic cell death? *Autophagy*. 8:1-3.
- Siegel, R., Naishadham, D., Jemal, A. (2013). Cancer statistics, 2013. *CA Cancer J Clin*. 63:11-30.
- Stanford, M.M., Shaban, M., Barrett, J.W., et al. (2008) Myxoma virus oncolysis of primary and metastatic B16F10 mouse tumors in vivo. *Mol Ther*. 16:52-59.
- Stojdl, D.F., Lichty, B.D, tenOever, B.R, Paterson, J.M, Power, A.T., Knowles, S. (2003). VSV strains with defects in their ability to shutdown innate immunity are potent systemic anti-cancer agents. *Cancer Cell*. 4:263-75.

- Su, M., Mei, Y., Sinha, S. (2013). Role of the crosstalk between autophagy and apoptosis in cancer. *J Oncol.* 2013:102735:102749.
- Tadros, N.N. and Garzotto, M. (2011). Androgen deprivation therapy for prostate cancer: Not so simple. *Asian J. Androl.* 13:187-188.
- Takaoka, A., Hayakawa, S., Yanai, H., Stoiber, D., Negishi, H., Kikuchi, H., Sasaki, S., Imai, K., Shibue, T., Honda, K., & Taniguchi, T. (2003). Integration of interferon-alpha/beta signaling to p53 responses in tumor suppression and antiviral defence. *Nature*,. 424:516-523.
- Taqi, A.M., Abdurrahman, M.B., Yakubu, A.M., Fleming, A.F. (1981). Regression of Hodgkin's disease after measles. *Lancet.* 1:1112.
- Terstegen L, Gatsios P, Ludwig S, Pleschka S, Jahnen-Dechent W, Heinrich PC, Graeve L. (2001). The vesicular stomatitis virus matrix protein inhibits glycoprotein 130-dependent STAT activation. *J Immunol.* 167:5209-5216.
- Thanos D, Maniatis T (1995). Virus induction of human IFN beta gene expression requires the assembly of an enhanceosome. *Cell.* 83:1091–1100.
- Tumilasci VF, Olieri S, Nguyen TL, Shamy A, Bell J, Hiscott J. (2008). Targeting the apoptotic pathway with BCL-2 inhibitors sensitizes primary chronic lymphocytic leukemia cells to vesicular stomatitis virus-induced oncolysis. *J Virol.* 82:8487-8499.
- Ververis, K., Hiong, A., Karagiannis, T.C., Licciardi, P.V. (2013). HDACIs: multitargeted anticancer agents. *Biologics.* 7:47-60.
- Wagner, R.R., Rose, J.K. (1996). *Fields Virology* (K. D. BN, Howley, P.M. Ed. 3rd Edition ed.). Philadelphia: Lipincott Raven Publishers.
- Wang, B.X. and Fish, E.N. (2012). The yin and yang of viruses and interferons. *Trends Immunol.* 33:190-197.
- Weichert, W. (2009). HDAC expression and clinical prognosis in human malignancies. *Cancer Lett.* 280:168–76
- Whelan, S.P. (2008). *Encyclopedia of Virology* (3rd ed.): London: Academic Press.
- White, E. (2012). Deconvoluting the context-dependent role for autophagy in cancer. *Nat Rev Cancer.* 12:401-410.
- Wilkins, A. and Parker, C. (2010). Treating prostate cancer with radiotherapy. *Nat Rev Clin Oncol.* 7:583-589.
- Wong, J., Zhang, J., Si, X., Gao, G., Mao, I., McManus, B.M., Luo, H. (2008). Autophagosome supports coxsackievirus B3 replication in host cells. *J Virol,* 82:9143-9153.

- Xu, W.S., Parmigiani, R.B., Marks, P.A. (2007). Histone deacetylase inhibitors: molecular mechanisms of action. *Oncogene*. 26:5541–52.
- Yap, T.A., Zivi, A., Omlin, A., de Bono, J.S. (2011). The changing therapeutic landscape of castration-resistant prostate cancer. *Nat Rev Clin Oncol*. 8:597-610.
- Yokoyama, T., Iwado, E., Kondo Y., et al. (2008). Autophagy-inducing agents augment the antitumor effect of telomerase-sense oncolytic adenovirus OBP-405 on glioblastoma cells. *Gene Ther*. 15:1233-9
- Yoneyama, M. and Fujita, T. (2009). RNA recognition and signal transduction by RIG-I-like receptors. *Immunol Rev*. 227:54–65.
- Yang, XJ and Seto E. (2008). The Rpd3/Hda1 family of lysine deacetylases: from bacteria and yeast to mice and men. *Nat Rev Mol Cell Biol*. 9:206-218.
- Yue, Z., Jin, S., Yang, C., Levine, A.J., Heintz, N. (2003). Beclin 1, an autophagy gene essential for early embryonic development, is a haploinsufficient tumor suppressor. *Proc Natl Acad Sci U S A*. 100:15077-15082.
- Ziparo, E., Petrungaro, S., Marini, E.S., Starace, D., Conti, S., Facchiano, A., Filippini, A., Giampetri, C. (2013). Autophagy in prostate cancer and androgen suppression therapy. *Int J Mol Sci*. 14:12090-12106.

CHAPTER 2

RESULTS

Manuscript I

Histone deacetylase inhibitors potentiate VSV oncolysis in prostate cancer cells by modulating NF- κ B signaling

This manuscript is currently in preparation for submission to the Journal of Virology.

Laura Shulak¹, Vladimir Beljanski², Cindy Chiang², Sucharita M. Dutta³, Julien Van Grevenynghe¹, S. Mehdi Belgnaoui¹, Thi Lien-Anh Nguyen¹, Thomas Di Lenardo¹, Rongtuan Lin¹, O. John Semmes³, and John Hiscott²

¹*Lady Davis Institute - Jewish General Hospital, McGill University, Montreal, CA*

²*Vaccine & Gene Therapy Institute of Florida, Port St. Lucie, FL*

³*The Leroy T. Canoles Jr Cancer Research Center, Eastern Virginia Medical School, Norfolk, VA*

Correspondence should be addressed to:

Dr. John Hiscott

Division of Infectious Diseases

VGTI Florida

9801 Discovery Way

Port St. Lucie FL 34987

Email: jhiscott@vgtifl.org

Rationale for Manuscript I

Though many cancer models are sensitive to the oncolytic activity of VSV-Δ51, several cell lines and primary tumors remain partially or completely refractory to oncolytic virotherapy. We have previously shown that combining VSV with the histone deacetylase inhibitors entinostat or vorinostat *in vitro*, in *in vivo* tumor models, and in primary *ex vivo* tumor explants resulted in enhanced viral replication, synergistic induction of cell death and reduced tumor growth with no adverse effects in healthy tissues. An unexpected but advantageous feature of this combination therapy was its reversibility. HDIs had to be administered continuously in order to maintain robust virus replication, indicating that this combination strategy requires effective protein hyperacetylation within the tumor to achieve maximal effective oncolytic activity. In order to elucidate which pathways modulated by vorinostat were responsible for enhancement of VSV oncolysis, we performed a genome-wide microarray analysis, taking advantage of the reversible nature of the treatment to focus in on key pathways. We found that continuous vorinostat treatment correlated with the upregulation of a subset of NF-κB target genes. We hypothesized that stimulation of the NF-κB pathway contributed to HDI-mediated enhancement of VSV replication and oncolysis. The aims of this study were to:

- 1) Characterize acetylation status and cellular localization of the NF-κB transcription factor subunit RelA/p65 upon vorinostat treatment
- 2) Assess VSV oncolytic ability with or without vorinostat treatment upon inhibition of NF-κB signaling
- 3) Identify which downstream effectors of NF-κB were responsible for vorinostat-mediated potentiation of VSV oncolysis

Abstract

Vesicular stomatitis virus (VSV) replication and oncolytic potential is reversibly stimulated in combination with epigenetic modulators such as the histone deacetylase inhibitor (HDI) Vorinostat. Based on this reversible effect of Vorinostat on viral oncolysis, we reasoned that critical host genes involved in oncolysis may be reversibly regulated in prostate cancer PC3 cells following removal of Vorinostat. A transcriptome analysis in PC3 cells identified a subset of NF- κ B target genes that were reversibly regulated by Vorinostat and involved in regulation of inflammatory and stress-responses. Consistent with the induction of NF- κ B target genes, Vorinostat-mediated enhancement of VSV oncolysis correlated with hyper-acetylation of the NF- κ B RELA/p65; furthermore, VSV replication and cell killing were suppressed when NF- κ B signaling was inhibited using pharmacological or genetic approaches. Additional bioinformatics analysis revealed that stimulation of NF- κ B signaling also resulted in the increased expression of several autophagy-related genes. Inhibition of autophagy by 3-methyladenine (3-MA) led to enhanced expression of IFN-stimulated genes, and both 3-MA treatment or genetic ablation of the key autophagy regulator Atg5 led to a decrease in VSV replication and oncolysis. Together, these data demonstrate that Vorinostat stimulates NF- κ B activity in a reversible manner via modulation of RELA/p65 signaling, leading to induction of autophagy and enhancement of VSV replication and oncolysis. These studies thus directly link NF- κ B signaling and autophagy with VSV replication and oncolysis.

Introduction

Oncolytic viruses (OV) are highly promising biotherapeutics that have demonstrated significant antitumor effects and safety in phases I-III clinical trials (1-3). Vesicular stomatitis virus (VSV) is an enveloped, negative-sense RNA virus of the *Rhabdoviridae* family that is a highly potent OV (4). It induces cell death primarily through activation of apoptotic pathway, and both intrinsic and extrinsic mechanisms have been described as contributors to VSV-induced apoptosis (5-7). Upon VSV infection, cytosolic nucleic acid sensing receptor activation leads to induction of the innate immune responses and production of interferons (IFNs). Newly synthesized IFN proteins act in both autocrine and paracrine manners leading to upregulation of IFN-stimulated genes and induction of antiviral response (8). Interferon-dependent responses play a major role in restricting VSV replication and are responsible for selective infection and lysis of tumor cells which frequently acquire diminished responsiveness to IFN effects (9-11). A small plaque variant VSV contains a D51 deletion in the viral matrix (M) protein; this mutation was shown to further enhance the safety profile of the virus (referred to as VSV from here on) (11, 12); the attenuated mutant is a potent inducer of the IFN response in healthy cells that does not block nuclear export of host cell antiviral mRNAs (11, 13, 14). A recombinant VSV expressing IFN β for increased selectivity is currently being tested in phase I clinical trials as a single agent in patients that are refractory to standard therapeutics (3).

Although preclinical and clinical studies utilizing OV in cancer treatment have generated highly promising data, several factors limit the efficacy of viral vectors, including intrinsic tumor resistance to oncolysis due to the residual innate immune

responses (11, 15, 16). For example, while VSV-based therapy was effective *in vivo* against androgen-dependent LNCaP prostate cancer xenograft model, androgen-independent PC3 cells were less susceptible to oncolysis both *in vitro* and *in vivo* (17). In contrast to LNCaP cells, PC3 cells possess mechanisms that are partially responsive to IFN, and these cells are refractory to VSV infection at low multiplicities of infection (MOIs). We previously characterized a synergistic strategy in prostate cancer that involves the use of histone deacetylase inhibitors (HDIs) such as suberoylanilide hydroxamic acid (SAHA, Vorinostat) or MS-275 together with oncolytic VSV in the treatment of androgen independent prostate cancer (16). HDIs manipulate innate immune response by influencing epigenetic modifications of chromatin and altering gene expression (18, 19). Because of their effect on immune suppression, we and others have reasoned that pre-treatment of tumors with HDIs would enhance the replication and spread of OV within malignancies (16, 20). In tumor cell lines, small animal tumor models, and in *ex vivo* primary tumor tissues, HDIs markedly enhanced the spread and replication of VSV. This increased oncolytic activity correlated with a time-dependent decrease in the expression of IRF3, IRF7, IFN β , and MX1, and increases in Caspase-3, -8 and -9 cleavages in Vorinostat + VSV and MS-274 + VSV treated PC3 cells (16). Interestingly, the effect of HDIs on viral spread was reversible, and removal of HDIs led to a decrease in viral replication within malignant cells both *in vitro* and *in vivo*.

Vorinostat has been shown to affect NF- κ B-related signaling pathways, inhibit IFN signaling, and induce cancer cell differentiation by inhibiting de-acetylation of cellular proteins and histones (16, 21, 22). Treatment of tumor cells with HDIs most frequently induces apoptosis via programmed apoptotic cell death through caspase activation (23). More recently, Vorinostat was shown to also induce autophagy in tumor cells (24, 25). Autophagy is a catabolic process by which cytosolic material is targeted

for lysosomal degradation by means of double-membrane cytosolic vesicles, termed autophagosomes [reviewed in (26)]. In addition to its role in cellular homeostasis, Autophagy also plays a critical role in the intrinsic, innate, and adaptive responses to pathogens, with evidence indicating that multiple viruses can either subvert or hijack the host autophagic machinery to support their own replication (27-29). A number of recent studies highlight the significant role of autophagy in mediating antitumor effects of oncolytic viruses, although the mechanism is largely unknown [reviewed in (30)].

The purpose of the present study was to elucidate the molecular mechanism(s) involved in the Vorinostat-mediated development of VSV permissiveness in PC3 cells. Our results demonstrate that Vorinostat not only blocks IFN responses, but also stimulates expression of a subset of NF- κ B target genes that enhances VSV replication in part via stimulation of NF- κ B mediated autophagy.

Results

Gene expression profiles in PC3 cells treated with VSV and Vorinostat. To determine genes and pathways responsible for HDI potentiation of VSV oncolysis, we performed total transcriptome analysis of PC3 cells exposed to the combination of VSV and Vorinostat. The effect of Vorinostat or MS-275 on both gene transcription and viral replication was reversible; upon removal of Vorinostat or MS-275, VSV replication decreased in PC3 cells, as previously demonstrated *in vivo* in different murine tumor models (16), and is illustrated by a 3-4 fold lower number of GFP-positive cells ($p < 0.05$) in wells where Vorinostat or MS-275 were removed prior to VSV-GFP infection (**Figure 1A**). Based on previous experiments, we reasoned that critical gene sets responsible for increased VSV replication would likewise be reversibly regulated by Vorinostat. To identify such genes, PC3 cells were treated with Vorinostat continuously (48h), or alternatively Vorinostat treatment was halted at the time of VSV infection (24h). In agreement with our previous results, we observed increases in the expression of IFN β and several IFN β -stimulated genes in VSV, VSV + Vorinostat (continuous), and VSV + Vorinostat (halted) groups (**Figure 1B**). However, the increase in such genes was most prominent in the “halted” group, in which the removal of Vorinostat activates antiviral response leading to a decrease in viral replication (**Figure 1A**). Additional bioinformatics analysis of gene expression profiles between treatment groups revealed a subset of reversibly regulated genes, many of which were well known NF- κ B targets (**Figure 1C**). Because expression of NF- κ B target genes was similar in Vorinostat or Vorinostat + VSV treated cells, NF- κ B activation appeared to be a direct consequence of Vorinostat treatment.

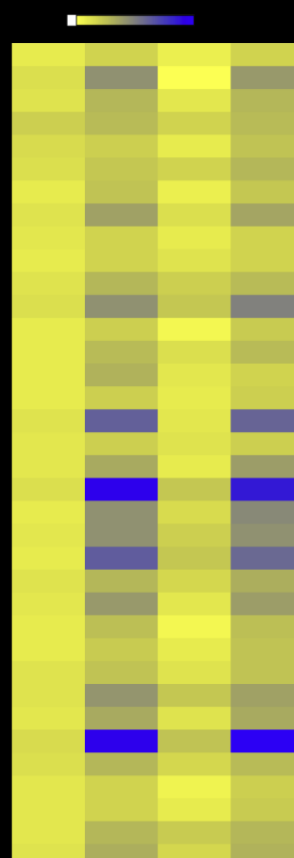
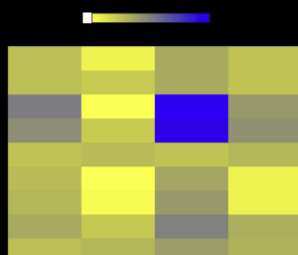
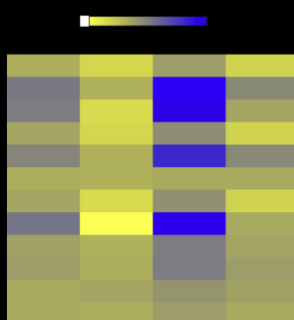
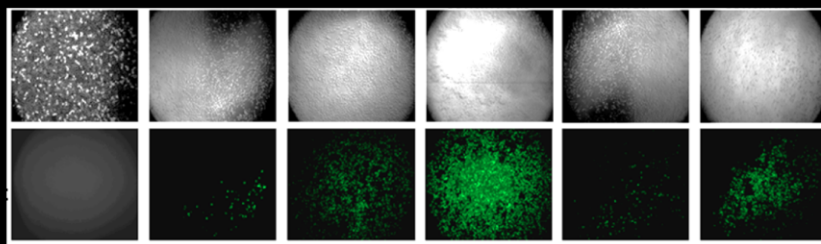


Figure 1: Vorinostat treatment potentiates VSV replication, induces expression of NF-kB regulated genes, and suppresses interferon response. A) PC3 cells were pretreated with MS-275 (2 μ M) or Vorinostat (5 μ M) for 24 h and then infected with VSV-GFP at MOI = 0.01. Following infection, culture media was either supplemented with complete media containing MS-275 or Vorinostat (continuous treatment) or complete media alone (halted treatment). VSV replication was assessed by fluorescence microscopy for GFP expression 24 h after VSV infection, and fluorescence signal was calculated for corrected total cell fluorescence (CTCF) using ImageJ; B) The heatmaps showing differentially regulated genes belonging to IFN signaling pathway (top) or Activation of IRF by cytosolic pattern recognition receptors (bottom). The genes were selected based on the Ingenuity Pathway Analysis gene assignment. C) The heatmap showing differentially regulated genes that are targets of NF-kB transcription factor, RELA/p65. * $P \leq 0.05$;

Vorinostat treatment increases chromatin binding and acetylation of RelA/p65.

Vorinostat treatment increases global protein acetylation [reviewed in (23)] and specifically targets acetylation of NF- κ B subunit RELA/p65, leading to increased nuclear localization and DNA binding (35). To evaluate the specific effect of Vorinostat or MS-275 on RELA/p65 activity, acetylation and DNA binding of RELA/p65 was evaluated (**Figure 2**). Immunoblot analysis of RELA/p65 revealed a modest but significant 1.3-2.2 fold increase in total acetylated lysine residues with continuous Vorinostat or MS-275 treatments ($p < 0.01$) (**Figure 2A** lanes 5 and 8). Chromatin fractionation also revealed a 1.7-2.4 fold increase in DNA binding of RELA/p65 following continuous treatment (**Figure 2B** lanes 5 and 7). Total I κ B α protein levels as an indirect measure of NF- κ B activity also displayed a higher turnover rate with continuous Vorinostat (2.2 fold higher) or MS-275 treatment (6 fold higher) ($p < 0.01$). The effect of Vorinostat on increased protein acetylation was confirmed by ~2 fold increases in the mean fluorescence intensity (MFI) for total acetylated histones and ~1.3-1.4 fold increases in MFI for acetylated K310 of RELA/p65 in Vorinostat- and Vorinostat + VSV-treated cells (**Figure 2C**). No increase in fluorescence intensities were observed in experiments using pan specific antibodies targeting histones 3 and 4 or RELA/p65 protein. To identify the RELA/p65 lysines acetylated as a consequence of Vorinostat treatment, S-tagged WT-RELA/p65 expressed in PC3 cells was analyzed by ESI-MS/MS mass spectrometry. Eight lysine residues - K56, K62, K122, K123, K195, K310, K314, K315 - demonstrated increased acetylation with Vorinostat, including K310 acetylation which is linked to increased transcriptional activity of RELA/p65 (36) (**Figure 2D**). These data indicate that Vorinostat treatment led to prolonged acetylation of eight of eighteen lysine residues in RELA/p65, resulting in increased nuclear localization and DNA binding.

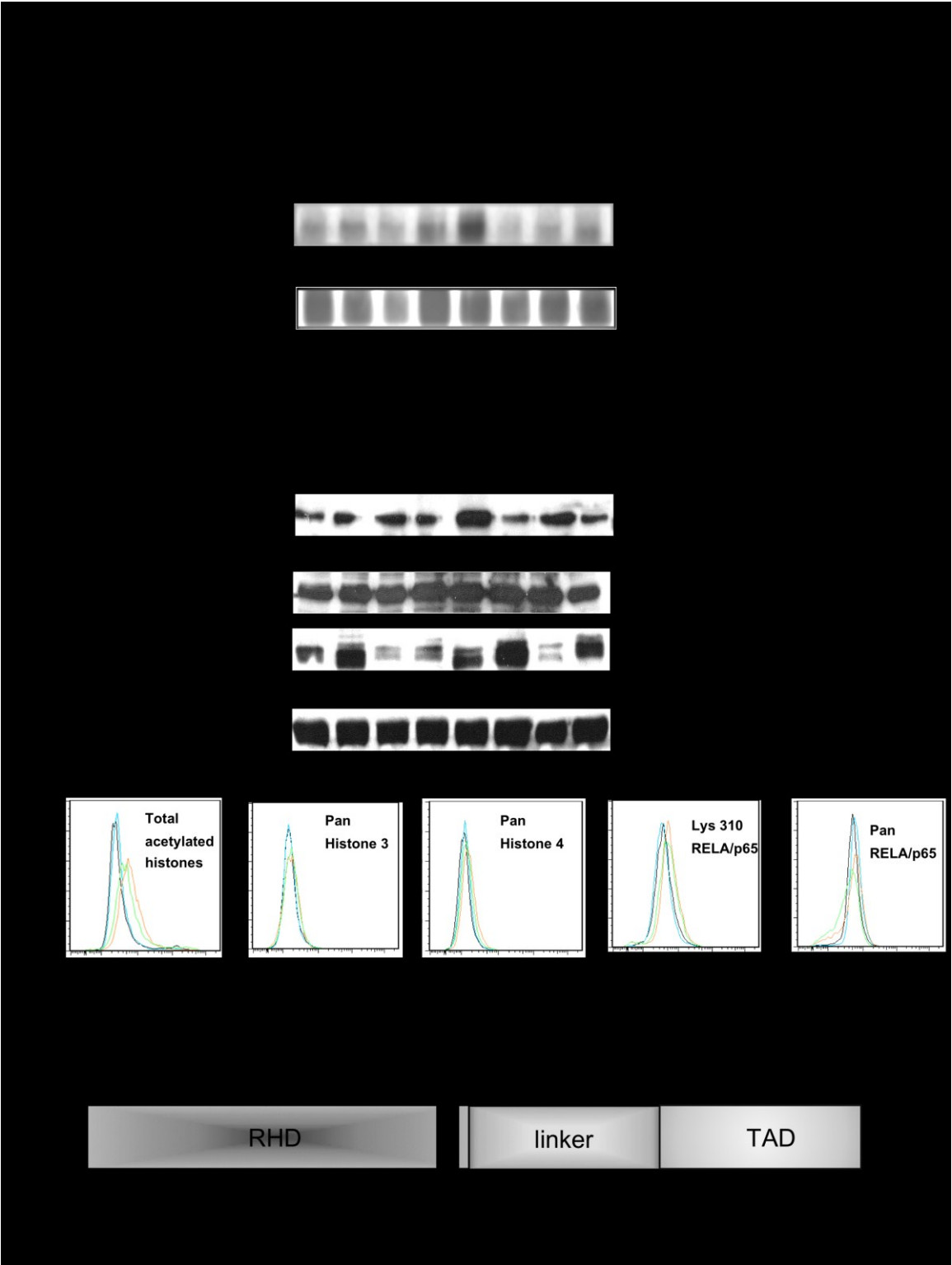


Figure 2 Legend: A) PC3 cells were exposed to the treatments indicated on top and nuclear extracts were immunoprecipitated for RelA/p65, and immunoblotted for acetylated lysine residues or total RelA/p65 protein. B) PC3 cells were subjected to the indicated experimental conditions for 24 hr. Chromatin-bound fraction was separated by gel electrophoresis and immunoblotted for RelA/p65. ORC2 was used as a loading control for chromatin bound-proteins (top panels). Proteins from whole cell lysates were immunoblotted for I κ B α (bottom panels). C) PC3 cells were exposed to VSV (MOI = 0.1) +/- Vorinostat (5 μ M) for 24 hr and intracellular staining was performed for total acetylated histones, or total Histone 3 and Histone 4 proteins (left panels); antibody targeting K310 of RelA/p65 or pan-RelA/p65 antibody were used for detection of acetylated lysine or total protein (right panels). D) Schematic representation of RelA/p65 with acetylated lysines as determined by mass spectrometry analysis indicated on the top. WCE-whole cell extract; C-continuous treatment; H-halted treatment; APC- allophycocyanin; RHD-Rel homology domain; TAD-transactivation domain; NLS-nuclear localisation signal.

NF- κ B inhibition blocks Vorinostat-induced RelA/p65 nuclear translocation and target gene expression. To further characterize the effect of NF- κ B signaling on VSV replication and RELA/p65 nuclear retention, a specific inhibitor of I κ B kinase (IKK), BAY11-7082, was used to block NF- κ B activity (37). Compared to control or VSV-treated cells (**Figure 3A**, lanes 1 and 3), a 3-6 fold increase ($p < 0.005$) in nuclear retention of RELA/p65 was observed in cells treated with Vorinostat or Vorinostat + VSV (**Figure 3A**, lanes 5 and 7). However, increased nuclear retention of RELA/p65 was reversed in cells treated with Vorinostat, VSV, and BAY11-7082, demonstrating that BAY11 efficiently inhibited RELA/p65 nuclear translocation/retention stimulated by Vorinostat + VSV treatment (**Figure 3A**, lane 9). By immunofluorescence, the combination of Vorinostat + VSV led to an 6-fold increase in the number of GFP-positive cells ($p < 0.01$) and in nuclear localization of RELA/p65, as indicated by higher nuclear signal for REL/p65 compared to control (**Figure 3B** white arrow); co-treatment with BAY11-7082 dramatically decreased the number of GFP-positive cells as well as the nuclear signal for RELA/p65 (**Figure 3B** right panel), indicating decreases in viral replication and nuclear retention of RELA/p65, respectively. The inhibitory effect of BAY11-7082 on NF- κ B target gene expression was also examined by measuring mRNA levels of several NF- κ B target genes (**Figure 3C**). While increased expression of I κ B α , IL1 β , CDKN1A, TNFAIP3, or BIRC3 mRNA was observed in cells treated with Vorinostat + VSV, co-treatment with BAY11-7082 led to ~50% decrease in expression of these genes ($p < 0.005$). Altogether, these data indicate that BAY11-7082 can efficiently decrease VSV replication, RELA/p65 nuclear retention, and NF- κ B target gene expression in PC3 cells.

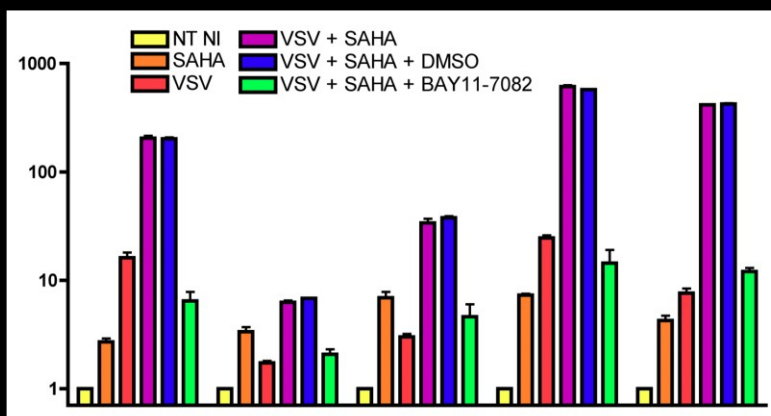
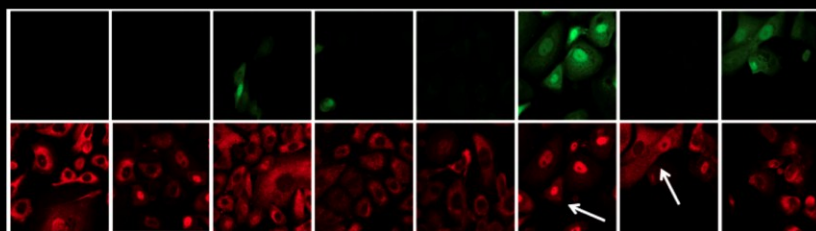


Figure 3 Legend: PC3 cells treated with VSV (MOI = 0.01) +/- Vorinostat for 24 hr were also pre-treated with 10 μ M BAY11-7082 for 1 hr where indicated. A) Nuclear (N) and cytosolic (C) extracts were separated by gel electrophoresis and immunoblotted for RelA/p65. THOC1 was used as a loading control for nuclear fraction; B) Confocal microscopy analysis of PC3 cells that were infected with VSV-GFP (green), treated as indicated and immunostained for RelA/p65 (red); C) Relative mRNA levels of several NF- κ B target genes in PC3 cells exposed to indicated treatments and assessed by qPCR.

Inhibition of NF- κ B signaling blocks Vorinostat-mediated enhancement of VSV replication. To determine the effect of NF- κ B inhibition on VSV replication and oncolysis, PC3 cells were infected with VSV-GFP in the presence of Vorinostat or MS-275 and BAY11-7082 (**Figure 4**). A ~50-70% decrease in the number of GFP-positive cells (**Figure 4A**) and 1-2 log decrease in virion release (**Figure 4B**) were observed in PC3 cells that were additionally treated with BAY11-7082. Cell viability, as measured by percentage of GFP, AnnexinV, and 7AAD triple negative cells, was also increased (~80%) with additional BAY11-7082 treatment compared to cells exposed to VSV + Vorinostat only.

We also examined the effects of decreased expression of RELA/p65 in PC3 cells on VSV replication using a genetic approach (**Figure 4D** and **4E**). PC3 cells stably transfected with LeGO-1xT vector expressing short hairpin RNA (shRNA) that targets expression of RELA/p65 (RELA-shRNA) or a control shRNA targeting expression of luciferase (Luc-Ctrl) (31), were infected with VSV and viral replication was measured by immunoblotting (data not shown), plaque assay (**Figure 4D**), and qPCR (**Figure 4E**). Knockdown of RELA/p65 efficiently inhibited VSV replication, as shown by a ~1 log decrease in VSV replication in the knockdown cells (white bars) compared to control cells (black bars). Pretreatment with Vorinostat did not rescue viral replication, indicating that the Vorinostat-mediated effect required functional NF- κ B signaling. Altogether, these data demonstrate that pharmacologic or genetic inhibition of NF- κ B signaling leads to a decrease in VSV replication and oncolysis, as well as an increase in cell survival.

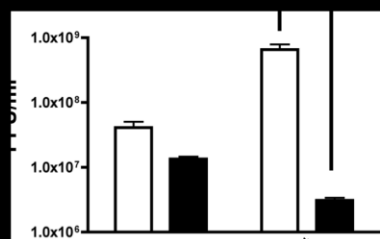
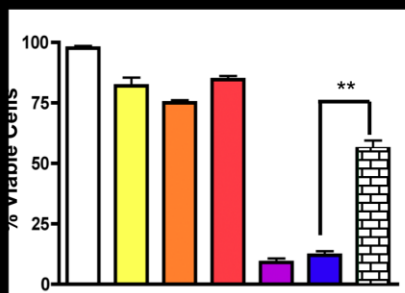
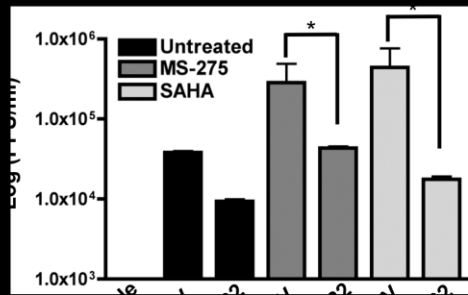
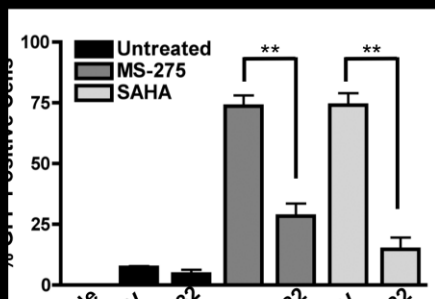


Figure 4 legend: BAY11-7082 or knockdown of RELA/p65 reverses Vorinostat or MS-275-mediated enhancement of VSV oncolysis. PC3 cells were pre-treated with DMSO (black bars), MS-275 (2 μ M) (dark grey bars) or Vorinostat (5 μ M) (light gray bars) +/- BAY11-7082 (10 μ M) and infected with VSV-GFP (MOI = 0.01) as indicated below graphs for 24 h. Viral replication was quantified by A) flow cytometry, or B) plaque assay; C) Cell viability of PC3 cells was measured by flow cytometry as percentage of GFP and Annexin-V double-negative cells. D) Quantification of VSV replication by plaque assay in Luc-Ctrl (black bars) and RELA-shRNA (white bars) cells exposed to VSV +/- Vorinostat; E) Quantification of VSV genomic mRNA by qPCR in Luc-Ctrl (white bars) and RELA-shRNA cells (black bars) exposed to VSV +/- Vorinostat at 12 and 24 h post-infection. * $P \leq 0.05$, ** $P \leq 0.01$; *** $P \leq 0.005$

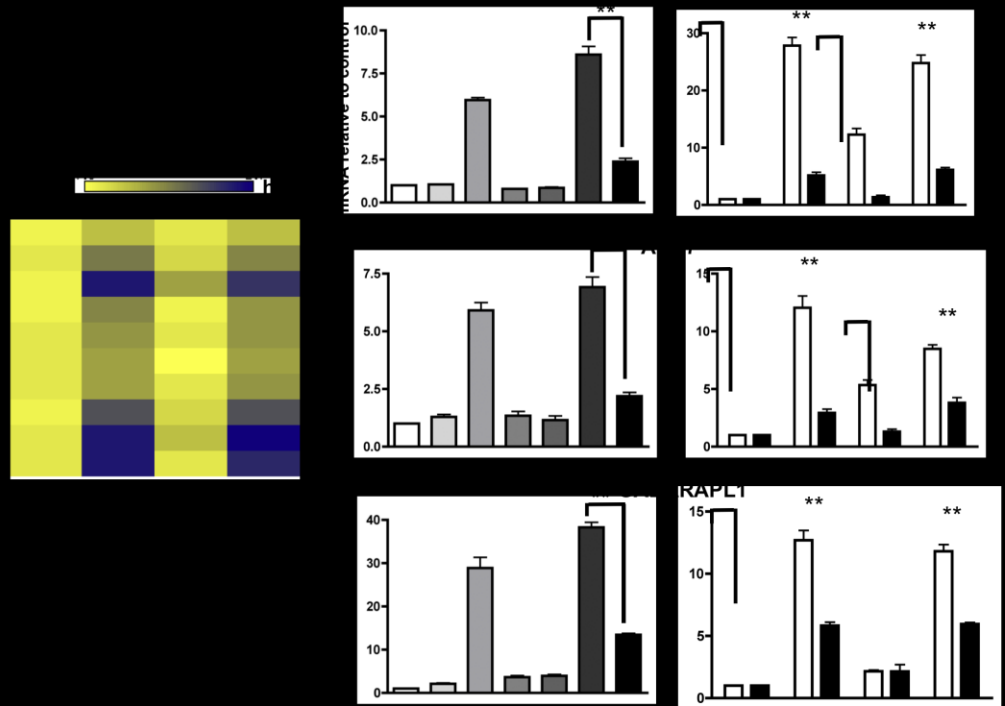
Vorinostat potentiates VSV oncolysis by increasing autophagy. To further investigate the mechanistic basis of NF- κ B-mediated potentiation of VSV oncolysis, we searched for potential downstream effectors of NF- κ B signaling. From the global expression data set, we identified increased expression (up to 2.7 fold) of genes that belong to the autophagy pathway in PC3 cells after treatment with Vorinostat alone or with Vorinostat + VSV (**Figure 5A**). Several of the autophagy-related genes (indicated with a star on **Figure 5A**) were found to possess one or more RELA/p65 binding motifs, based on a search of their promoter regions (www.genecards.org, Weizmann Institute, Rehovot, Israel). In agreement with this observation, the levels of mRNA for ATG101, ATG7 and GABARAPL1 increased 6-30 fold in mRNA in PC3 cells exposed to Vorinostat or Vorinostat + VSV, whereas a ~4 fold decrease ($p < 0.01$) was observed following co-treatment with BAY11-7082 (**Figure 5B** left panels). Furthermore, expression of ATG101, ATG7 and GABARAPL1 were 2-5 fold lower in Vorinostat- or Vorinostat + VSV-treated cells stably knocked down for RELA/p65 (white bars) compared to control (black bars) (**Figure 5B** right panels).

RELA-shRNA or Luc ctrl PC3 cells were also examined for induction of autophagy by Cyto-ID staining (38) and for apoptosis by annexin V staining at 24 or 48h after exposure to VSV +/- Vorinostat (**Figure 5C**). At 24 h, Vorinostat alone or Vorinostat + VSV treatments increased the number of Cyto-ID-positive Luc-Ctrl cells (75-83 %) (white bars). In contrast, only a slight increase in the number of Cyto-ID-positive cells were observed in RELA-shRNA cells exposed to Vorinostat or Vorinostat + VSV (~15 %) (light grey bars). Only ~6 % increase in annexin V-positive cells at 24 h was observed in Luc-Ctrl cells upon Vorinostat or VSV + Vorinostat treatment. In contrast, at 48h post-infection, ~66 % of Luc-Ctrl cells (dark grey bars) compared to ~15 % of RELA-shRNA cells (black bars) were annexin V-positive. At this time point, <10% of Luc Ctrl cells (dark grey bars) and ~35% of RELA shRNA cells were Cyto-ID-positive. Taken together, these data indicate that induction of autophagy markers in Luc Ctrl cells. Knockdown of RELA/p65 by shRNA, on the other hand, impairs induction of both autophagy and apoptosis.

To further confirm the role of autophagy in Vorinostat-mediated increase in VSV cytotoxicity, autophagy-deficient mouse embryonic fibroblasts (Atg5^{-/-} MEFs), were infected with VSV in the presence of increasing concentrations of Vorinostat (**Figure 6A**). While addition of Vorinostat led to increased VSV replication in wt MEFs, no

increase in VSV replication was observed upon addition of Vorinostat to Atg5^{-/-} MEFs (**Figure 6A**). Furthermore, in PC3 cells, addition of the autophagy inhibitor 3-methyladenine (3-MA) led to a decrease in the number of GFP-positive cells even in the presence of Vorinostat (**Figure 6B**). Because autophagy plays a role in innate immune response to viral infections (39), we evaluated expression of several innate antiviral response genes using a Fluidigm BioMarkTM assay (**Figure 6C**). Treatment with 3-MA in the presence of Vorinostat increased the mRNA levels of IFN-stimulated genes, CXCL10, IFIT1, IFIT2, IFITM1, MX1 and MX2, in VSV-infected cells, indicating that autophagy inhibition increased IFN antiviral responses. The increase in mRNA was specific for IFN β regulated genes as no increase in the levels of pro-inflammatory IL1A, IL6 or IL10 genes were observed. The reversal of immunosuppressive effects of Vorinostat by 3-MA were further confirmed by immunoblotting for IFIT1, MX1, and ISG15 in PC3 cells. Upregulation of the three proteins was observed in cells that were treated with VSV + Vorinostat + 3-MA compared to cells that were treated only with VSV + Vorinostat (**Figure 6D**). Taken together, these data demonstrate that functional autophagy plays a major role in Vorinostat-mediated increase in VSV replication by decreasing IFN-mediated antiviral responses.

We further confirmed the role of NF- κ B signaling in VSV oncolysis using two additional VSV resistant cell lines, prostate cancer DU145 and colon cancer HCT116, as well as two VSV permissive cell lines, breast cancer MCF-7 and prostate cancer 22Rv1 cells (**Figure 7**). Decreases in cell survival and increased virion release were observed in DU145 (white bars) and HCT116 cells (black bars) upon VSV + Vorinostat treatment compared to VSV infection alone (**Figure 7A** and **7B**). Addition of BAY11-7082 increased cell survival and decreased viral replication by approximately 2 log-fold. In agreement, treating permissive MCF-7 cells with BAY11-7082 (**Figure 7C**), or transfecting of 22Rv1 cells with a dominant-negative form of I κ Ba (**Figure 7D**) all led to a decrease in VSV replication. To assess whether Vorinostat treatment induces autophagy in DU145 and HCT116 cells, we examined two markers of autophagy, LC3 cleavage and degradation of SQSTM1 (40) (**Figure 7E**). In either cell line, Vorinostat treatment alone or in combination with VSV induced LC3 cleavage and degradation of SQSTM1, indicating activation of the autophagic pathway.



c)

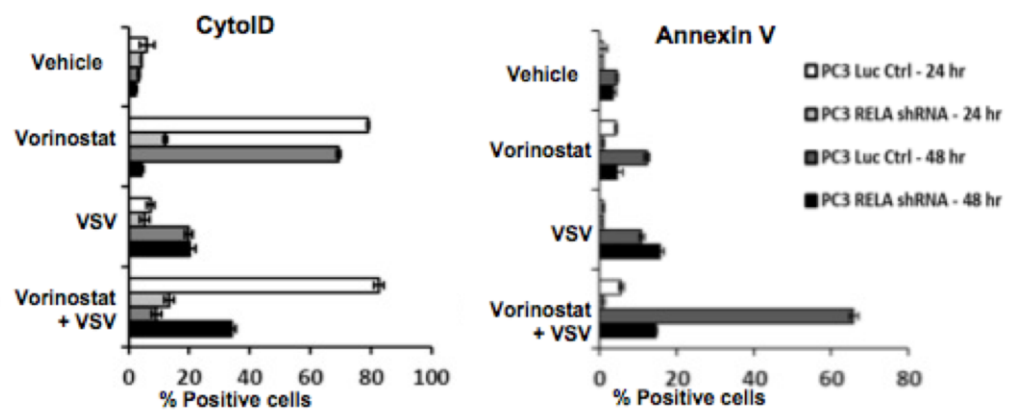


Figure 5 legend: Vorinostat treatment upregulates the autophagy pathway. A) Fold changes of autophagy-related genes assessed by global genome expression profiling in four experimental groups relative to non-treated (control) PC3 cells; B) qPCR assessment of mRNA levels for ATG101, ATG7 and GABARAPL1 genes in PC3 cells exposed to VSV (MOI = 0.01) +/- Vorinostat (5 μ M) in the presence of BAY11-7082 (10 μ M) (left panels) or in Luc-Ctrl and RELA-shRNA PC3 cells exposed to VSV +/- Vorinostat for 24 h (right panels) - black bars indicate Luc ctrl and white bars RELA-shRNA PC3 cells. C) Luc-Ctrl or RELA-shRNA stably transfected PC3 cells were treated with VSV +/- Vorinostat for 24 h or 48 h; the levels of autophagic vesicles or apoptosis were measured by flow cytometry using the Cyto-ID® Autophagy Detection Kit or annexin V staining, respectively. White bars indicate 24 h treated Luc-Ctrl cells, light gray bars indicate 24 h treated RELA-shRNA cells, dark gray bars indicate 48 h treated Luc-Ctrl cells, and black bars indicate 48 h treated RELA-shRNA cells. H = halted; C= continuous. ** $P \leq 0.01$

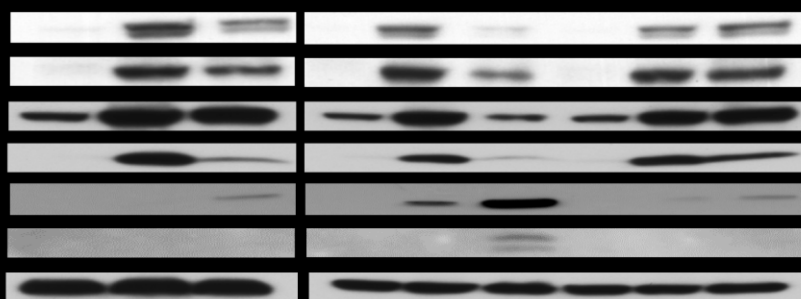
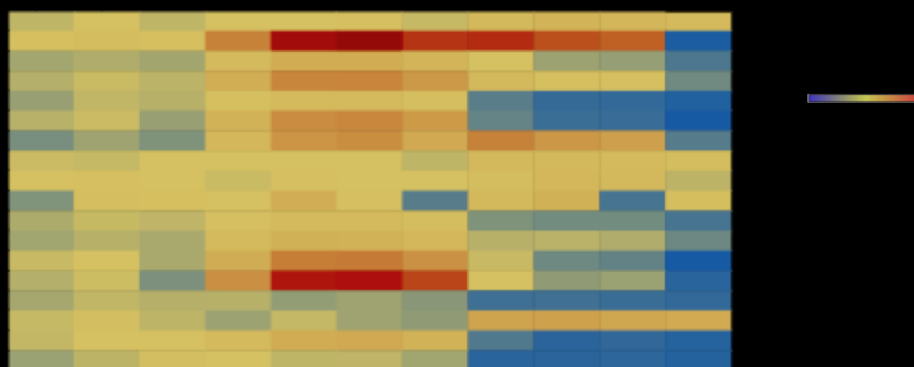
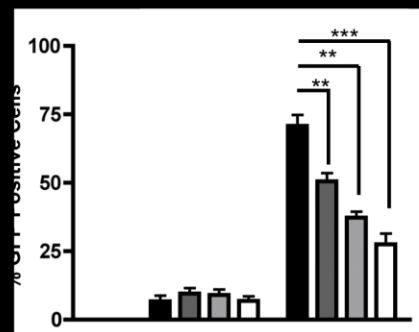
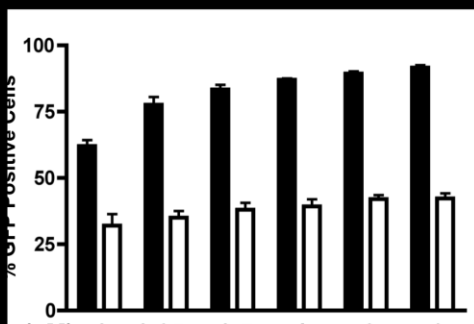


Figure 6 legend: Inhibition of autophagy decreases VSV replication and increases antiviral signaling. A) Atg5^{+/+} (black bars) or Atg5^{-/-} (white bars) MEFs were exposed to the indicated concentrations of Vorinostat, infected with VSV-GFP (MOI = 0.0001), and viral replication was assessed 24 h later by flow cytometry; B) PC3 cells were treated with 0 μ M (black bars), 5 μ M (dark grey bars), 7.5 μ M (light gray bars), or 10 μ M (white bars) of 3-methyladenine (3-MA) for 1 h prior to VSV-GFP (MOI = 0.01) infection and viral replication was assessed by flow cytometry 24 h later; C) Gene expression analysis using Dynamic Arrays platform for several genes (indicated on the left) in PC3 cells exposed to VSV (MOI = 0.01), Vorinostat (5 μ M) +/- 5, 7.5, or 10 μ M 3-MA. D) PC3 cells were exposed to treatments indicated on top, and antiviral signaling was assessed by immunoblotting. ** $P \leq 0.01$; *** $P \leq 0.005$

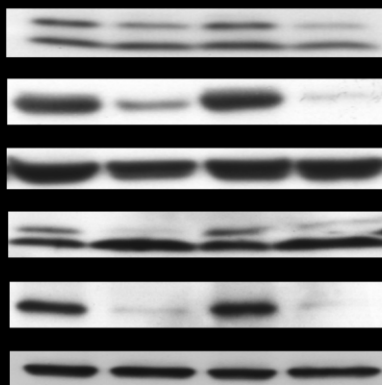
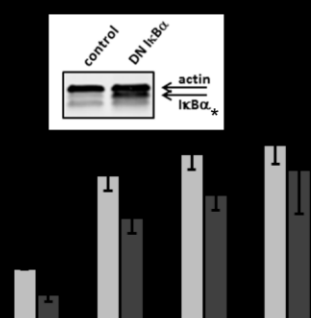
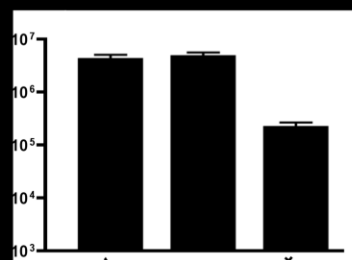
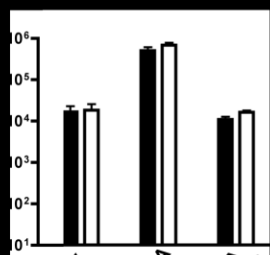
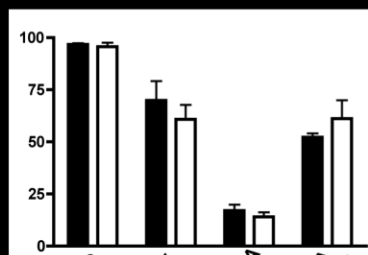


Figure 7 legend: Vorinostat promotes VSV replication and induces autophagy in non-permissive cells. A) DU145 or HCT116 cells were exposed to VSV +/- 5 μ M SAHA in combination with 10 μ M BAY11-7082 where indicated for 24 hr. Cell viability was measured by flow cytometry as percentage of GFP and annexin V double-negative cells and B) VSV replication was assessed by plaque assay; C) MCF-7 cells were exposed to VSV (MOI = 0.0001) +/- BAY11-7082 (5 μ M) and plaque assay was used to assess VSV replication; D) 22Rv1 cells were exposed to the indicated MOIs of VSV and the effect of a transient transfection with a dominant-negative (DN) I κ B α on VSV replication was measured by plaque assay; E) DU145 and HCT116 cells were exposed to the treatments indicated above and autophagy markers were assessed by immunoblotting.

Discussion

Biotherapeutics such as OV vectors represent a novel and promising approach to cancer treatment. Numerous OVs are currently being tested in pre-clinical and clinical trials; among those, VSV is an attractive OV because it is a potent inducer of apoptosis in cancer cells (4). VSV-induced apoptosis involves activation of Caspase-8, Fas death receptor pathway, as well as PKR (41). However, some tumor cell lines and many primary tumors are resistant to OVs due to partially preserved innate immune responses. In previous studies, we and others (16, 42-44) characterized a combination strategy using HDIs to potentiate oncolysis in cancer cells that are not highly permissive to OV replication. However, the antitumor mechanism of such therapeutic combinations remained elusive, and in the present study, we sought to investigate the molecular aspects of oncolysis. We demonstrate that Vorinostat in combination with VSV: 1) induces reversible expression of IFN β -stimulated and a subset of NF- κ B regulated genes; 2) induces hyperacetylation and increases nuclear retention of RelA/p65; 3) increases expression of autophagy-related genes; and 4) triggers both autophagy and apoptosis in prostate cancer cells.

Global genome expression analysis of differentially regulated genes in PC3 cells exposed to Vorinostat +/- VSV revealed changes in the expression of IFN β -regulated genes; increased expression of numerous NF- κ B-regulated genes were also observed in Vorinostat-treated cells. Subsequent biochemical analysis revealed increased acetylation and nuclear retention of NF- κ B subunit RELA/p65 in the presence of Vorinostat and mass spectrometry analysis of RELA/p65 identified acetylation of eight lysine residues in RELA/p65. The functional role for several acetylated lysines of RELA/p65 are known: acetylation of K310 is required for full transcriptional activity (36), acetylation

of K314 and K315 regulates specificity of gene expression (45) and acetylation of K122 and K123 reduces DNA binding capacity (46). We also detected for the first time increased acetylation of K56, K62, and K195, although the functional role(s) for these sites are currently unknown. Based on our data, these lysines may play a role in nuclear shuttling, sequestration, and/or regulation of DNA binding affinity.

Further bioinformatics analysis of differentially regulated genes revealed increased expression of several autophagy-related genes in PC3 cells after treatment with Vorinostat or Vorinostat + VSV. This observation led us to further examine the connection between NF- κ B and autophagy. Increased expression of three autophagy-related genes - ATG101, ATG7 and GABARAPL1 – was observed in cells where NF- κ B signaling was stimulated with Vorinostat; conversely, inhibition of NF- κ B by BAY11-7082 or shRNA-mediated knockdown of RELA/p65 led to decreased expression of ATG101, ATG7 and GABARAPL1. The role of autophagy in viral infection is context-dependent and may involve elimination of viral particles, or suppression of apoptosis and/or innate immune responses providing suitable environment for viral replication. Stimulation of pattern recognition receptors induces autophagy by unknown mechanisms, and autophagy may also be a mechanism by which viruses and other pathogens escape innate immune responses (39). Autophagy can also contribute to oncolysis; for example, a combination of oncolytic adenovirus and autophagy inducers greatly improved OV antitumor efficacy in both glioblastoma cell lines and U87MG-derived glioma xenograft models (49). We also previously described a role for autophagy as an antitumor mechanism in chronic lymphocytic leukemia cells (CLL) where treatment of CLL cells with the combination of Bcl-2 inhibitors and VSV led to induction of metabolic stress and subsequent disruption of anti-autophagic protein-protein interactions (50).

Activation of the canonical NF- κ B pathway is also closely associated with regulation of autophagy. TGF β -activated kinase 1 (TAK1) activates IKK which in turn phosphorylates I κ B α , the inhibitory subunit of the NF- κ B complex, leading to activation of NF- κ B-mediated signaling. If TAK1 or any other component of the IKK complex is inhibited, induction of autophagy by upstream stimuli is impaired (48). Although the main function of NF- κ B is to regulate the expression of specific genes in the cells of immune system, some viruses can utilize anti-apoptotic properties of NF- κ B and divert its function from regulation of immune responses to modulation of cells growth and apoptosis which gives viruses a survival advantage [reviewed in (47)].

In the present manuscript, we demonstrate that Vorinostat indirectly upregulates autophagy by inducing acetylation and increased nuclear retention of RelA/p65 leading to an upregulation of several autophagy-related genes. Further evaluation of Vorinostat-mediated mechanisms revealed that autophagy precedes apoptosis in VSV + Vorinostat treated cells and autophagy appears to contribute to VSV oncolysis via suppression IFN-dependent immune responses. Vorinostat-mediated potentiation of VSV replication was also observed in wt MEFs but not in autophagy-deficient Atg5^{-/-} cells. Furthermore, decreased VSV replication was observed even in the presence of Vorinostat when autophagy was inhibited with 3-MA. Mechanistically, treatment of PC3 cells with 3-MA led to upregulation of the IFN β -stimulated genes even in the presence of Vorinostat, suggesting that autophagy facilitates VSV replication by decreasing antiviral signaling. These data are in agreement with *Jounai et al.* who reported that in MEFs, autophagy proteins constitutively associate with RIG-I and MAVS proteins and thus restrict virus-induced type I IFN response (51).

In summary, we provide new evidence that Vorinostat potentiates VSV oncolysis not only by direct suppression of innate immune responses but also by indirectly

stimulating induction of the autophagic pathway via activation of NF- κ B. With a number of OV entering clinical trials and promising data emerging from Phases II and III clinical trials (3, 52), understanding the cellular processes that modulate tumor responses to virus-based therapies becomes an essential component of the successful clinical implementation of OVs.

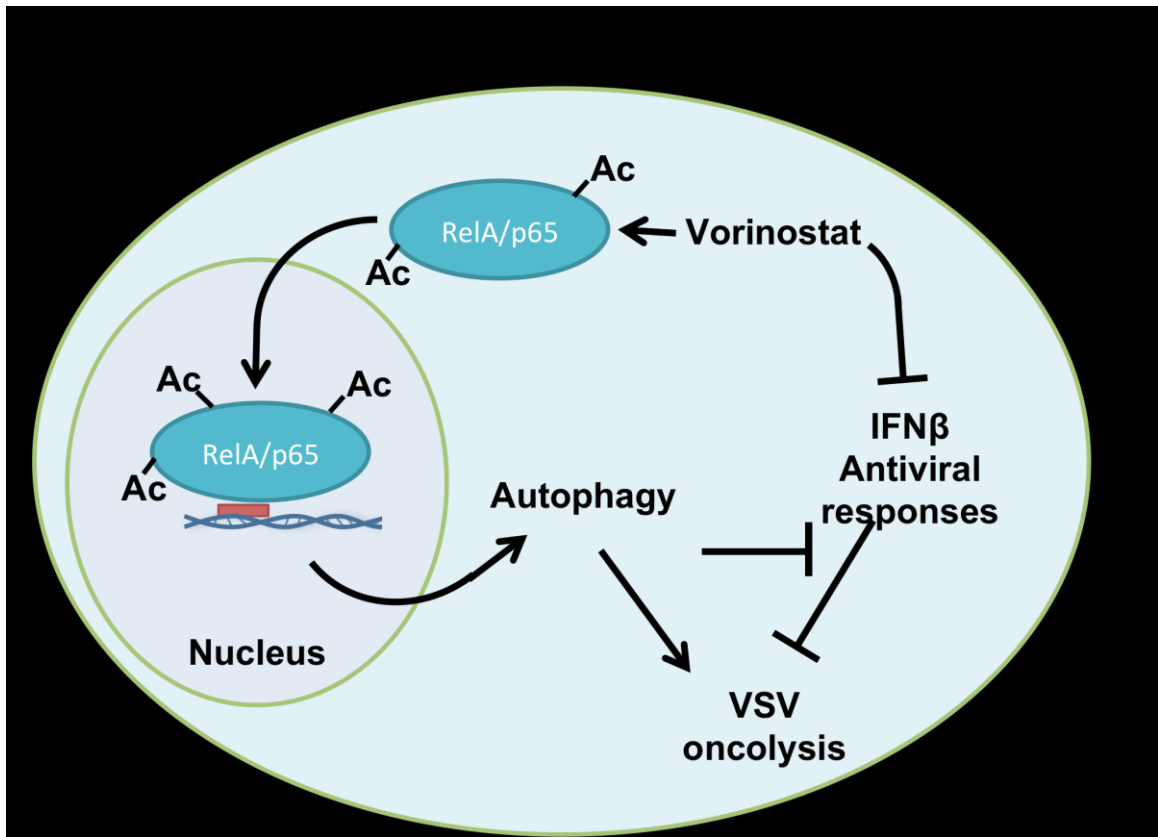


Figure 8 Legend: Vorinostat induces both suppression of IFN β signaling and hyperacetylation of RelA/p65 (unknown whether this occurs primarily in cytosol, nucleus, or both) resulting in its nuclear translocation and increased nuclear retention. Nuclear RelA/p65 induces expression of several autophagy-related genes and upregulation of autophagy allows for increased VSV replication and oncolysis by further suppression of IFN β signaling and possible other unknown mechanisms . Ac – acetylated lysines.

Acknowledgments

We would like to thank Dr. David Olnagier for critical reading of the manuscript, and Dr. Antony Cooper for help with histone acetylation experiments. This work was supported by grants from the Fondation de Recherches en Santé de Québec, Canadian Institutes of Health Research (MOP 42562). Terry Fox Foundation with the support of the Canadian Cancer Society, and the Department of Defense grant LC110658 to J.H. The authors declared no conflict of interest.

Materials and Methods

Cell lines and reagents. PC3, DU145, and HCT116 cells were purchased from ATCC (Bethesda, MD) and were grown in RPMI (PC3), EMEM (DU145), or McCoy's (HCT116) supplemented with 10 % serum (Life Technologies, Carlsbad, CA). Atg5 wild-type (WT) (Atg5^{+/+}) and Atg5 knockout (KO) (Atg5^{-/-}) mouse embryonic fibroblasts (MEFs) were obtained from Dr. Nathalie Grandvaux, CRCHUM-Centre Hospitalier de l'Université de Montréal, Montréal, CA, with the permission of Dr. Noboru Mizushima, who generated the original Atg5 WT and KO MEFs. PC3 cells stably transfected with shRNA targeting luciferase control (PC3 Luc Ctrl) or RelA/p65 (PC3 RELA-shRNA) were a kind gift from Dr. Thorsten Schinke, University Medical Center Hamburg Eppendorf, Hamburg, DE. Vorinostat, MS-275, and BAY11-7082 were purchased from Cayman Chemicals (Ann Arbor, Michigan). Human TNF α recombinant protein was purchased from eBiosciences (San Diego, CA). 3-methyladenine and all other chemicals were purchased from Sigma-Aldrich (St Louis, MO).

Virus production, quantification and infection. VSV stock was grown in Vero cells (ATCC, Bethesda, MD), concentrated from cell-free supernatants by centrifugation and titrated in duplicate by standard plaque assay. PC3, DU145, or HCT116 cells were infected at various multiplicities of infection (MOIs) and incubated with complete medium at 37 °C for the indicated times.

Immunoprecipitation. Twenty micrograms of anti-RelA/p65 (Santa Cruz Biotechnology, Santa Cruz, CA) were crosslinked to 300 μ l of Protein AG-Plus agarose beads using 0.2 mol/l triethanolamine pH 8.0. Cells were lysed with 1% CHAPS lysis buffer (10 mmol/l HEPES, 150 mM NaCl, 1% CHAPS, pH 7.4) containing protease inhibitors and total protein was incubated with crosslinked antibody in 1% CHAPS lysis buffer at 4°C overnight. Immunoprecipitates were collected by centrifugation and washed three times with 1% CHAPS lysis buffer, beads were boiled in loading buffer and bound protein was analyzed by immunoblotting. Samples with antibody alone, lysate alone, or with an irrelevant isotype-matched immunoglobulin G antibody were used as negative controls. Proteins were separated by electrophoresis and transferred to

nitrocellulose membrane. Acetylated lysine (Cell Signaling Technologies, Danvers, MA) and RelA/p65 (Santa Cruz Biotechnology, Santa Cruz, CA) antibodies were used .

Isolation of cellular chromatin fraction. Approximately 3×10^6 cells were rinsed twice with ice cold PBS and harvested with a cell scraper into 1 ml ice-cold PBS. The cells were centrifuged at 1500 rpm for 2 minutes, the supernatant discarded, and the cell pellet resuspended in ice-cold PBS. The cells were again centrifuged and the pellet resuspended in 200 μ l of buffer A (100 mM HEPES, pH 7.9, 10 mM KCl, 1.5 mM MgCl_2 , 0.34 M Sucrose, 10% glycerol, 10 mM NaF, 1 mM Na_2VO_3 , 1 mM DTT and protease inhibitor cocktail) with a blunt 1000 μ l micropipet tip. Triton X-100 was added to a final concentration of 0.1% incubated on ice for 5 minutes. The solution was then centrifuged at 1,300 g (4000 rpm) at 4°C for 5 minutes in a 1.5 ml centrifuge tube. The supernatant (fraction S1) was separated from the pellet (fraction P1), which contains the nuclei. Fraction S1 was cleared by high-speed centrifugation at 20,000 g (14,000 rpm) at 4°C for 5 minutes. The supernatant (fraction S2), which represents the cytosolic fraction, was collected and the pellet was discarded. Fraction S2 was stored at -80°C until ready to use. Pellet fraction P1 was washed once with buffer A (0.6 ml per tube) by centrifugation again at 4000 rpm at 4°C for 5 minutes. Washed fraction P1 was resuspended in 100 μ l of buffer B (3 mM EDTA, 0.2 mM EGTA, 1 mM DTT, protease inhibitor cocktail) with blunt 1000 μ l micropipet tip and lysed for 30 minutes on ice. The P1 sample was then centrifuged at 1,700 g (5000 rpm) at 4°C for 5 minutes. The resulting supernatant (fraction S3), which contains the soluble nuclear proteins, was separated from the pellet (fraction P2) that contains the chromatin. Fraction S3 was stored at -80°C until ready to use. Fraction P2 was washed once with Buffer B (0.6 ml per tube) by centrifugation at 10,000 g (11,000 rpm) at 4°C for 1 minute. Fraction P2 was then resuspended in 1% NP-40 protein extraction buffer (180 μ l per sample), briefly sonicated and clarified by high-speed centrifugation at 20,000 g (14,000 rpm) at 4°C for 5 minutes. The final supernatant (fraction P3), which contains the chromatin bound proteins, was collected and kept at -80°C until ready to use.

Protein extraction and Western blot analysis. Cells were washed twice with ice-cold phosphate buffered saline and lysed in buffer (50 mM Tris-HCl, pH 8, 1% sodium deoxycholate, 1 % NP-40, 5 mM EDTA, 5 mM EGTA and 150 mM NaCl), and the

insoluble fraction was removed by centrifugation at 22,000 x g for 20 min. The soluble fractions were separated by SDS-PAGE on 10 % gels. Proteins were electrophoretically transferred to a PVDF membrane, blocked with 10 % bovine serum albumin and probed with various primary antibodies. All immunoblots were visualized by enhanced chemiluminescence. Protein concentration was determined with Bio-Rad protein assay reagent (BioRad, Hercules, CA). Protein extracts were resolved using mini 16 PROTEAN TGX precast gels (BioRad, Hercules, CA) and transferred to polyvinylidene difluoride membrane.

Mass spectrometry analysis. PC3 cells were transfected with an empty vector or S-tagged WT-RelA/p65, then treated with Vorinostat (5 μ M) for 48 hr. S-tagged protein was then precipitated using the S-tag purification technique as described previously (5), resolved on SDS-PAGE, fixed and stained with Coomassie Brilliant Blue. RelA/p65 in-gel Reduction, Alkylation, Denaturation and Trypsin Digestion: The corresponding protein bands were excised, de-stained and washed with a series of three washing buffers (50 mM ammonium bicarbonate, 50 % acetonitrile and 80 % acetonitrile). The bound proteins were reduced with 1 ml of 40 mM dithiothreitol for 25 min at 56 °C. The gels were rinsed with 1 ml of 50 mM ammonium bicarbonate buffer and the reduced proteins were alkylated with 1 ml of 50 mM Iodoacetamide for 30 min at 25 °C in the dark with constant mixing. The Iodoacetamide was discarded and the gel bound proteins were digested with 0.5 ml of trypsin (20 ng/ μ l; Promega, Madison, WI) in 50 mM ammonium bicarbonate buffer at 37°C with constant mixing for 12h. After digestion, the tryptic fraction was collected, and the gels were washed with 50mM ammonium bicarbonate to collect any remaining tryptic peptides. The eluent containing the tryptic peptides were dried using a Speed-Vac apparatus (Thermo Fisher Scientific, San Jose, CA) and stored at 4 °C prior to mass spectrometric analysis. Peptide/Protein Identifications by ESI-MS/MS analysis: The dried samples were dissolved with 20 μ l of 0.1 % formic acid/water. 2 μ l of each sample was analyzed by LC/ESI-MS/MS using a Q-Exactive (Thermo Fisher Scientific, San Jose, CA) mass spectrometer with an Easy NanoLC-1000 system using data dependent acquisition with dynamic exclusion (DE = 1) settings. The data dependent acquisition settings used were a top 12 higher energy collision induced dissociation (HCD) for the Q-Exactive MS. Resolving power for Q-Exactive was set at 70,000 for the full MS scan, and 17,500 for the MS/MS scan at m/z

200. LC/ESI-MS/MS analysis was conducted using a C18 column (75 μ m x 150mm). The mobile phases for the reverse phase chromatography were (A) 0.1% HCOOH in water and (B) 0.1% HCOOH in acetonitrile. A four-step, linear gradient was used for the LC separation (2% to 30% B in the first 47 minutes, followed by 80%B in the next 1 minute and holding at 80% B for 12 minutes). The Sequest algorithm was used to identify peptides from the resulting MS/MS spectra by searching against the combined human protein database (a total of 22,673 proteins) extracted from Swissprot (version 57) using taxonomy “homo sapiens” using Proteome Discoverer (version 1.3, Thermo Fisher Scientific, San Jose, CA). Searching parameters for parent and fragment ion tolerances were set as 20 ppm and 30 mmu for the Q Exactive MS. Other parameters used were a fixed modification of carbamidomethylation –Cys, variable modifications of acetylation (K) and oxidation (Met). Trypsin was set as the protease with a maximum of 2 missed cleavages. Raw files were searched against RelA protein (3 different isoforms) (along with 500 other random proteins and reversed proteins as decoys) using Byonic (6) with a peptide tolerance of 15 ppm; an MS/MS tolerance of 20 ppm for HCD data; the carbamidomethylated cysteine as fixed modification and oxidation of methionine and acetylation (K) as variable modifications. Byonic scoring gives an indication of whether modifications are confidently localized.

Nuclear Extraction. Cells ($1-2 \times 10^7$) were washed and harvested with cold PBS with 1mM EDTA. Cell pellet was resuspended in ice cold buffer A (10 mM Tris pH 7.9, 10 mM KCL, 0.1 mM EDTA, 0.1 mM EGTA, 1mM DTT) for 15 min and 25 ml of 10 % NP-40 was added. Cell suspension was vortexed for 15 sec, and after 2 min spin at 13,300 g supernatant (cytosolic fraction) was separated from the pellet (nuclear fraction). Nuclear fraction was further solubilized by resuspending of pellet in 50 ml of cold buffer C (20 mM Tris, 400 mM NaCl, 1 mM EDTA, 1 mM EGTA, pH 7.9) and shaking vigorously at 4 °C for 1 hour; insoluble debris was removed by a 15 min spin (13,300 g) at 4 °C.

Autophagy analysis by flow cytometry. Autophagy was assessed by Cyto-ID staining by flow cytometry (LSRFortessa, BD Biosciences, San Jose, CA). Cyto-ID was used according to the manufacturer's instructions (Enzo Life Sciences, Farmingdale, NY).

Confocal microscopy. PC3 cells were seeded onto 22-mm diameter coverslips in 6-well plates at 1×10^5 cells/well. Cells were washed twice with PBS and fixed in 4% paraformaldehyde for 15 minutes, washed 3 times with PBS and permeabilized with methanol for 2 minutes. Coverslips were blocked with 3% BSA/PBS for one hour at room temperature, incubated with primary antibody in 3% BSA/PBS overnight at 4°C, and washed twice in PBS/0.1% Tween20, and twice again in PBS. Coverslips were then incubated in secondary antibody (Alexa Fluor 546, Life Technologies, Carlsbad, CA) for one hour at room temperature followed by 2 washes in 3% BSA/PBS and 2 washes in PBS. Coverslips were mounted onto slides using Immu-Mount (Thermo Scientific, Waltham, MA), and left to dry overnight at room temperature in the dark.

Real-time RT-PCR analysis. Total RNA was isolated using RNeasy kit as per manufacturer's instructions (Qiagen, Valencia, CA). RNA (400 ng) was reverse transcribed with Oligo dT primers and SuperScript II reverse-transcriptase (Life Technologies, Carlsbad, CA). Five percent of RT reaction was used as template for PCR using Taq polymerase (GE Healthcare, Piscataway Township, NJ), amplification was carried for 25–30 cycles. All data are presented as a relative quantification with efficiency correction based on the relative expression of target genes versus β -actin as reference gene. Complementary DNA was amplified using SyBR Green I PCR master mix (Applied Biosystems, Foster City, CA) and the data was collected using the AB 7500 Real-Time PCR System and analyzed by Comparative CT Method using the SDS v1.3.1 Relative Quantification Software. For the FluidigmBioMark™ assay, intron-spanning PCR primers and probes were designed using Roche's Universal Probe Library Assay Design Center (www.universalprobelibrary.com). The standard BioMark™ protocol was used to preamplify cDNA samples for 14 cycles using TaqMan® PreAmp Master Mix per the manufacturer's protocol (Applied Biosystems, Foster City, CA). qPCR reactions were performed using 96.96 BioMark™ Dynamic Arrays (Fluidigm, South San Francisco, CA) enabling quantitative measurement of up to 96 different mRNAs in 96 samples under identical reaction conditions. Runs were 40 cycles (15 seconds at 95°C, 5 seconds at 70°C, 60 seconds at 60°C). Raw CT values were calculated by the Real-Time PCR Analysis Software (Fluidigm) and software-designated failed reactions were discarded from analysis. The following primers were used:

IL1 β : F:5'-GCACGATGCACCTGTACGAT-3', R:5'-

AGACATCACCAAGCTTTTTTGCT-3';
IκBα:F:5'GATCACCAACCAGCCAGAAATT3',R:5'TCTCGGAGCTCAGGATCAC
A3';*CDKN1A*:F:5'CCTCATCCCGTGTTCCTTT3'R:5'GTACCACCCAGCGGAC
AAGT-3';*TNFAIP3*:F:5'-ACCCATTGTTCTCGGCTAT-3'R:5'-
CGGTCTCTGTTAACAAGTGGAA-3';*BIRC3*: F:5'-
TGTTGGGAATCTGGAGATGA-3'R:5'-CGGATGAACTCCTGTCCTTT-
3';*VSV*:F:5'-TTGGCAAGTATGCTAAGTCAG-3'-,R:5'-
CACGTTATCCACCTCCGACT-3'GACTTGAGATACTCACGAA-3'; *ATG101*: F:5'-
GAAGTGTGGACGGTCAAGGT-3';*ATG7*:F:5'-AGGAGATTCAACCAGAGACC-
3',R:5'-GCACAAGCCCAAGAGAGG-3'*GABARAP1*: F:5'-
TGTCAGGACAGAGCTGTTGG-3', R:5'-CAAAGAGAAGGGAGCACAGG-3'.

Transfections. PC3 cells were cultured in RPMI-1640 medium supplemented with 10% fetal bovine serum. When the cells reached 60% to 70% confluence, cells were treated with Vorinostat and S-tagged RelA/p65 was transfected using Eugene6 reagent (Promega, Madison, WI), according to the manufacturer's instructions. After 24 hr, cells were infected with VSV for 24 hr, then harvested 24 hr later.

Intracellular staining. PC3 cells were exposed to VSV +/- Vorinostat for 48 hr. Cells (2×10^5) were fixed in Fix I buffer (BD Biosciences, San Jose, CA) for 10 min at 37 °C. Cells were washed with PBS containing 4% FBS and resuspended in Perm II buffer (BD Biosciences, San Jose, CA) for 30 min at 4 °C. After washing, cells were stained with 1 mg/100 ml of primary antibody for 30 min at room temperature, washed twice and incubated with 1.5 mg/200 ml of Alexa Fluor 647-conjugated anti-rabbit IgG (Jackson ImmunoResearch, West Grove, PA) for 25 min at room temperature. After two more washes, samples were analyzed by flow cytometry.

Statistical analysis. Graphics and statistical analysis were executed using GraphPad Prism 5 software (GraphPad Software, La Jolla, CA). Differences among the treatment groups were analyzed by paired t-test. The P values < 0.05 were considered statistically significant. Average values were expressed as mean \pm SD. FluidigmBioMark™ assay data were analyzed and Z scores were generated by Microsoft Excel.

Microarray analyses. PC3 cells were either untreated and uninfected, or treated with VSV, Vorinostat or combination (halted or continuous) and total RNA was isolated from samples (n = 4 per treatment group) using RNeasy Micro Kits (Qiagen, Valencia, CA). Universal human reference RNA was used as a reference. The quantity of the RNA was confirmed using a NanoDrop 2000c (Thermo Scientific, Waltham, MA) and quality was confirmed using an Agilent 2100 Bioanalyzer. Samples (50 ng) were then amplified using Illumina TotalPrep RNA amplification kits (Life Technologies, Carlsbad, CA). The microarray analysis was conducted using 750 ng of biotinylated complementary RNA hybridized to Human ref 8 version 3 BeadChips (Illumina, San Diego, CA) at 58 °C for 20 h. The arrays were scanned using Illumina's iSCAN and quantified using Genome Studio (Illumina, San Diego, CA). The analysis of the GenomeStudio output data was conducted using the R and Bioconductor software packages. A Significance Analysis of Microarray (SAM) test was then performed on each experimental condition vs. control. SAM identifies statistically significant genes by carrying out gene specific t-tests and computes a statistic d_j for each gene j , which measures the strength of the relationship between gene expression and a response variable. This analysis uses non-parametric statistics, since the data may not follow a normal distribution. The response variable describes and groups the data based on experimental conditions. In this method, repeated permutations of the data are used to determine if the expression of any gene is significant related to the response. The use of permutation-based analysis accounts for correlations in genes and avoids parametric assumptions about the distribution of individual genes. This generated a list of differentially expressed gene wherein we inputted a threshold of +1.3/-1.3 fold change and p value less than or equal to 0.01 to be considered significant. A manual search using Boston University's NF-kB target gene database (<http://www.nf-kb.org>) was then conducted to create a list of differentially regulated NF-kB target genes. Quantile normalization was applied, followed by a log2 transformation. The LIMMA package was used to fit a linear model to each probe and perform (moderated) t tests or F tests on the groups being compared. To control the expected proportions of false positives, the FDR for each unadjusted P value was calculated using the Benjamini and Hochberg method implemented in LIMMA. Multidimensional scaling was used as a dimensionality reduction method in R to generate plots for the evaluation of similarities or dissimilarities between datasets. Ingenuity Pathway Analysis software (IPA,

Ingenuity Systems, Redwood City, CA) was used to annotate genes and rank canonical pathways. Canonical pathways analysis identified the pathways from the IPA library of pathways that were most significant to the data set. Molecules from the data set that met the cutoff of 1.3, $p < 0.05$, and were associated with a canonical pathway in the Ingenuity Knowledge Base were considered for the analysis. The significance of the association between the data set and the canonical pathway was measured by determining of a ratio between the number of molecules from the data set that map to the pathway divided by the total number of molecules that map to the canonical pathway is displayed. Fisher's exact test was used to calculate a p-value determining the probability that the association between the genes in the dataset and the canonical pathway is explained by chance alone.

References

1. Rowan, K. 2010. Oncolytic viruses move forward in clinical trials. *J Natl Cancer Inst* 102:590-595.
2. Breitbach, C. J., J. Burke, D. Jonker, J. Stephenson, A. R. Haas, L. Q. Chow, et al. 2011. Intravenous delivery of a multi-mechanistic cancer-targeted oncolytic poxvirus in humans. *Nature* 477:99-102.
3. Russell, S. J., K. W. Peng, and J. C. Bell. 2012. Oncolytic virotherapy. *Nat Biotechnol* 30:658-670.
4. Hastie, E., and V. Z. Grdzlishvili. 2012. Vesicular stomatitis virus as a flexible platform for oncolytic virotherapy against cancer. *J Gen Virol* 93:2529-2545.
5. Cary, Z. D., M. C. Willingham, and D. S. Lyles. 2011. Oncolytic vesicular stomatitis virus induces apoptosis in U87 glioblastoma cells by a type II death receptor mechanism and induces cell death and tumor clearance in vivo. *J Virol*.
6. Pearce, A. F., and D. S. Lyles. 2009. Vesicular stomatitis virus induces apoptosis primarily through Bak rather than Bax by inactivating Mcl-1 and Bcl-XL. *J Virol* 83:9102-9112.
7. Gaddy, D. F., and D. S. Lyles. 2005. Vesicular stomatitis viruses expressing wild-type or mutant M proteins activate apoptosis through distinct pathways. *J Virol* 79:4170-4179.
8. Honda, K., H. Yanai, A. Takaoka, and T. Taniguchi. 2005. Regulation of the type I IFN induction: a current view. *Int Immunol* 17:1367-1378.
9. Barber, G. N. 2004. Vesicular stomatitis virus as an oncolytic vector. *Viral Immunol* 17:516-527.
10. Lichty, B. D., A. T. Power, D. F. Stojdl, and J. C. Bell. 2004. Vesicular stomatitis virus: re-inventing the bullet. *Trends Mol Med* 10:210-216.
11. Stojdl, D. F., B. D. Lichty, B. R. tenOever, J. M. Paterson, A. T. Power, S. Knowles, et al. 2003. VSV strains with defects in their ability to shutdown innate immunity are potent systemic anti-cancer agents. *Cancer Cell* 4:263-275.
12. Stojdl, D. F., B. Lichty, S. Knowles, R. Marius, H. Atkins, N. Sonenberg, et al. 2000. Exploiting tumor-specific defects in the interferon pathway with a previously unknown oncolytic virus. *Nat Med* 6:821-825.

13. Faria, P. A., P. Chakraborty, A. Levay, G. N. Barber, H. J. Ezelle, J. Enninga, et al. 2005. VSV disrupts the Rae1/mrnp41 mRNA nuclear export pathway. *Mol Cell* 17:93-102.
14. Barber, G. N. 2005. VSV-tumor selective replication and protein translation. *Oncogene* 24:7710-7719.
15. Russell, S. J., and K. W. Peng. 2007. Viruses as anticancer drugs. *Trends Pharmacol Sci* 28:326-333.
16. Nguyen, T. L., H. Abdelbary, M. Arguello, C. Breitbach, S. Leveille, J. S. Diallo, et al. 2008. Chemical targeting of the innate antiviral response by histone deacetylase inhibitors renders refractory cancers sensitive to viral oncolysis. *Proc Natl Acad Sci U S A* 105:14981-14986.
17. Ahmed, M., S. D. Cramer, and D. S. Lyles. 2004. Sensitivity of prostate tumors to wild type and M protein mutant vesicular stomatitis viruses. *Virology* 330:34-49.
18. Nguyen, T. L., M. G. Wilson, and J. Hiscott. 2010. Oncolytic viruses and histone deacetylase inhibitors--a multi-pronged strategy to target tumor cells. *Cytokine Growth Factor Rev* 21:153-159.
19. Glozak, M. A., and E. Seto. 2007. Histone deacetylases and cancer. *Oncogene* 26:5420-5432.
20. Katsura, T., S. Iwai, Y. Ota, H. Shimizu, K. Ikuta, and Y. Yura. 2009. The effects of trichostatin A on the oncolytic ability of herpes simplex virus for oral squamous cell carcinoma cells. *Cancer Gene Ther* 16:237-245.
21. Pei, X. Y., Y. Dai, and S. Grant. 2004. Synergistic induction of oxidative injury and apoptosis in human multiple myeloma cells by the proteasome inhibitor bortezomib and histone deacetylase inhibitors. *Clin Cancer Res* 10:3839-3852.
22. Suliman, B. A., D. Xu, and B. R. Williams. 2012. HDACi: molecular mechanisms and therapeutic implications in the innate immune system. *Immunol Cell Biol* 90:23-32.
23. New, M., H. Olzscha, and N. B. La Thangue. 2012. HDAC inhibitor-based therapies: can we interpret the code? *Mol Oncol* 6:637-656.
24. Gammoh, N., D. Lam, C. Puente, I. Ganley, P. A. Marks, and X. Jiang. 2012. Role of autophagy in histone deacetylase inhibitor-induced apoptotic and nonapoptotic cell death. *Proc Natl Acad Sci U S A* 109:6561-6565.
25. Lee, Y. J., A. J. Won, J. Lee, J. H. Jung, S. Yoon, B. M. Lee, et al. 2012. Molecular mechanism of SAHA on regulation of autophagic cell death in tamoxifen-

resistant MCF-7 breast cancer cells. *International journal of medical sciences* 9:881-893.

26. Choi, A. M., S. W. Ryter, and B. Levine. 2013. Autophagy in human health and disease. *N Engl J Med* 368:651-662.
27. Kirkegaard, K. 2009. Subversion of the cellular autophagy pathway by viruses. *Curr Top Microbiol Immunol* 335:323-333.
28. Kudchodkar, S. B., and B. Levine. 2009. Viruses and autophagy. *Reviews in medical virology* 19:359-378.
29. Dreux, M., and F. V. Chisari. 2010. Viruses and the autophagy machinery. *Cell Cycle* 9:1295-1307.
30. Meng, S., J. Xu, Y. Wu, and C. Ding. 2013. Targeting autophagy to enhance oncolytic virus-based cancer therapy. *Expert Opin Biol Ther* 13:863-873.
31. Schulze, J., K. Weber, A. Baranowsky, T. Streichert, T. Lange, A. S. Spiro, et al. 2012. p65-Dependent production of interleukin-1beta by osteolytic prostate cancer cells causes an induction of chemokine expression in osteoblasts. *Cancer Lett* 317:106-113.
32. Belgnaoui, S. M., S. Paz, S. Samuel, M. L. Goulet, Q. Sun, M. Kikkert, et al. 2012. Linear ubiquitination of NEMO negatively regulates the interferon antiviral response through disruption of the MAVS-TRAF3 complex. *Cell host & microbe* 12:211-222.
33. Bern, M., Y. Cai, and D. Goldberg. 2007. Lookup peaks: a hybrid of de novo sequencing and database search for protein identification by tandem mass spectrometry. *Anal Chem* 79:1393-1400.
34. Burgess, A., S. Vigneron, E. Brioudes, J. C. Labbe, T. Lorca, and A. Castro. 2010. Loss of human Greatwall results in G2 arrest and multiple mitotic defects due to deregulation of the cyclin B-Cdc2/PP2A balance. *Proc Natl Acad Sci U S A* 107:12564-12569.
35. Greene, W. C., and L. F. Chen. 2004. Regulation of NF-kappaB action by reversible acetylation. *Novartis Found Symp* 259:208-217; discussion 218-225.
36. Chen, L. F., Y. Mu, and W. C. Greene. 2002. Acetylation of RelA at discrete sites regulates distinct nuclear functions of NF-kappaB. *Embo J* 21:6539-6548.
37. Lee, J., M. H. Rhee, E. Kim, and J. Y. Cho. 2012. BAY 11-7082 is a broad-spectrum inhibitor with anti-inflammatory activity against multiple targets. *Mediators Inflamm* 2012:416036.

38. Chan, L. L., D. Shen, A. R. Wilkinson, W. Patton, N. Lai, E. Chan, et al. 2012. A novel image-based cytometry method for autophagy detection in living cells. *Autophagy* 8:1371-1382.
39. Richetta, C., and M. Faure. 2013. Autophagy in antiviral innate immunity. *Cell Microbiol* 15:368-376.
40. Klionsky, D. J., E. H. Baehrecke, J. H. Brumell, C. T. Chu, P. Codogno, A. M. Cuervo, et al. 2011. A comprehensive glossary of autophagy-related molecules and processes (2nd edition). *Autophagy* 7:1273-1294.
41. Gaddy, D. F., and D. S. Lyles. 2007. Oncolytic vesicular stomatitis virus induces apoptosis via signaling through PKR, Fas, and Daxx. *J Virol* 81:2792-2804.
42. Alvarez-Breckenridge, C. A., J. Yu, R. Price, M. Wei, Y. Wang, M. O. Nowicki, et al. 2012. The histone deacetylase inhibitor valproic acid lessens NK cell action against oncolytic virus-infected glioblastoma cells by inhibition of STAT5/T-BET signaling and generation of gamma interferon. *J Virol* 86:4566-4577.
43. Mactavish, H., J. S. Diallo, B. Huang, M. Stanford, F. Le Boeuf, N. De Silva, et al. 2010. Enhancement of vaccinia virus based oncolysis with histone deacetylase inhibitors. *PLoS One* 5:e14462.
44. Watanabe, T., M. Hioki, T. Fujiwara, M. Nishizaki, S. Kagawa, M. Taki, et al. 2006. Histone deacetylase inhibitor FR901228 enhances the antitumor effect of telomerase-specific replication-selective adenoviral agent OBP-301 in human lung cancer cells. *Exp Cell Res* 312:256-265.
45. Buerki, C., K. M. Rothgiesser, T. Valovka, H. R. Owen, H. Rehrauer, M. Fey, et al. 2008. Functional relevance of novel p300-mediated lysine 314 and 315 acetylation of RelA/p65. *Nucleic Acids Res* 36:1665-1680.
46. Kiernan, R., V. Bres, R. W. Ng, M. P. Coudart, S. El Messaoudi, C. Sardet, et al. 2003. Post-activation turn-off of NF-kappa B-dependent transcription is regulated by acetylation of p65. *J Biol Chem* 278:2758-2766.
47. Hiscott, J., T. L. Nguyen, M. Arguello, P. Nakhaei, and S. Paz. 2006. Manipulation of the nuclear factor-kappaB pathway and the innate immune response by viruses. *Oncogene* 25:6844-6867.
48. Niso-Santano, M., A. Criollo, S. A. Malik, M. Michaud, E. Morselli, G. Marino, et al. 2012. Direct molecular interactions between Beclin 1 and the canonical NFkappaB activation pathway. *Autophagy* 8:268-270.
49. Alonso, M. M., H. Jiang, T. Yokoyama, J. Xu, N. B. Bekele, F. F. Lang, et al. 2008. Delta-24-RGD in combination with RAD001 induces enhanced anti-glioma effect via autophagic cell death. *Mol Ther* 16:487-493.

50. Samuel, S., V. Beljanski, J. Van Grevenynghe, S. Richards, F. Ben Yebdri, Z. He, et al. 2013. BCL-2 Inhibitors Sensitize Therapy-resistant Chronic Lymphocytic Leukemia Cells to VSV Oncolysis. *Mol Ther* 21:1413-1423.
51. Jounai, N., F. Takeshita, K. Kobiyama, A. Sawano, A. Miyawaki, K. Q. Xin, et al. 2007. The Atg5 Atg12 conjugate associates with innate antiviral immune responses. *Proc Natl Acad Sci U S A* 104:14050-14055.
52. Patel, M. R., and R. A. Kratzke. 2013. Oncolytic virus therapy for cancer: the first wave of translational clinical trials. *Translational research : the journal of laboratory and clinical medicine* 161:355-364.

CHAPTER 3

DISCUSSION

3.1 Oncolytic virotherapy

Cancer is a diverse, heterogeneous disease that necessitates novel approaches to therapeutic strategies. OVs constitute a promising option in the development of these future strategies; not only do they target the tumor directly, but they also indirectly cause tumor cell death by inflammatory cytokine release, shutdown of tumor vasculature, and triggering adaptive immune responses, all without the debilitating side effects of current conventional chemotherapies (Kirn and Thorne, 2009). However, as is the case with most cancer treatment modalities, multiple aspects must be considered to provide the best treatment strategy. In order to take full advantage of the benefits of OV therapy, combination treatments targeting multiple features are likely to be the most effective. In the pursuit to establish rational, multi-pronged therapies, several studies have independently shown the value of combining oncolytic viruses with histone deacetylase inhibitors. HDIs are able to promote tumor-specific replication and oncolysis for at least six different oncolytic viruses (Nguyen *et al.*, 2008; Otsuki *et al.*, 2008; Katsura *et al.*, 2009; Vanoosten *et al.*, 2006; Watanabe *et al.*, 2006). The HDIs used in these studies are varied, and act upon different classes of HDACs, indicating that these compounds have a wide range of effects on viral oncolysis. The most obvious benefit of HDI treatment is the inhibition of the IFN antiviral response, which overcomes residual intra-tumoral innate immunity and allows for the replication and spread of OVs (Nguyen *et al.*, 2008; Otsuki *et al.*, 2008). It should be noted that the use of immunosuppressants is not without risks, which may encompass unwanted viral replication in healthy tissue or heightened susceptibility to viral infection. It appears from the evidence to date however, that the effect of HDIs on viral oncolysis is exquisitely selective for transformed cells. The reversibility of HDI treatment also

diminishes the possibility of these risks; since HDIs must be administered continuously in order for OV replication to occur, they can be used as chemical switches to adjust antiviral responses and control OV growth. This presents an important advantage in the future clinical application of OV combination therapies (Nguyen *et al.*, 2008). Elucidating all possible mechanisms of OV/HDI synergy is an important task in moving this combination therapy from the bench to the bedside, and it was to this end that this study was undertaken.

3.2 Vorinostat stimulates NF-kB signaling and target gene upregulation

The effect of HDI treatment on NF-kB signaling appears to be of a dual nature, with some groups reporting inhibition of NF-kB (Huang *et al.*, 1997; Inan *et al.*, 2000; Kramer *et al.*, 2001) and many others reporting the exact opposite (Adam *et al.*, 2003; Ashburner *et al.*, 2001; Quivy *et al.*, 2002). Results of this study agree with the latter, as we have demonstrated that vorinostat treatment hyperacetylates the RelA/p65 transcription factor subunit, and this correlates with increased nuclear retention and chromatin binding. Mass spectrometry analysis of RelA/p65 isolated from vorinostat-treated PC3 cells revealed acetylation at eight lysine residues. While the functional role of five of these acetylation sites is known (Buerki *et al.*, 2008; Chen *et al.*, 2002; Kiernan *et al.*, 2003), we have shown novel acetylation sites at three other lysine residues: K56, K62 and K195. Based on our data, these lysines may play a role in nuclear shuttling, sequestration, and/or regulation of DNA binding affinity, and it will be an interesting avenue for further study.

Consequent to activation of NF-kB, vorinostat treatment upregulates a number of NF-kB target genes. Unsurprisingly, as acetylation of RelA/p65 plays a role in dictating

specificity of gene expression (Buerki *et al.*, 2008), only a subset of the large number of known NF- κ B regulated genes were found to be induced. Inhibition of NF- κ B, via pharmacological and genetic approaches, was found to dramatically reduce HDI-mediated enhancement of VSV oncolysis in several cancer cell lines. These results indicate that intact NF- κ B signaling, and more specifically, acetylation-mediated activation of the RelA/p65 transcription factor subunit is required for HDIs to promote virus replication and oncolysis.

In our search for the downstream effectors responsible, we narrowed in on a group of autophagy related genes that were also upregulated by vorinostat treatment. Though future studies are needed to confirm that these are in fact regulated by NF- κ B, the majority of them were found to contain one or more RelA/p65 binding sites in their promoter regions. Indeed, inhibition of NF- κ B blocked both HDI-mediated induction of these genes, and HDI-mediated induction of autophagy, suggesting that the activation of autophagic signaling by VSV and vorinostat combination treatment occurs in an NF- κ B dependent fashion.

It is interesting to note that HDI-mediated activation of NF- κ B is often considered a hindrance in terms of the utility of HDIs as anticancer therapies. NF- κ B is generally thought of as anti-apoptotic, and its activation often leads to attenuated lethality in tumor cells. Many studies have been undertaken combining HDIs with NF- κ B inhibitors in an attempt to overcome this limitation (Duan *et al.*, 2007; Abaza *et al.*, 2012; Yao *et al.*, 2012; Dai *et al.*, 2011). In the case of OV combination treatment however, we and others (Katsura *et al.*, 2009) have demonstrated that stimulation of NF- κ B by HDIs sensitizes cancer cells to the intended apoptotic stimulus, the OV.

A potential risk factor of activating NF- κ B in tumor cells is linked to its association with inflammation-related tumorigenesis, and the possibility of triggering unwanted

inflammatory responses in healthy tissues (Karin, 2006; Chaturvedi *et al.*, 2010). It appears however, that as HDI treatment is specific to transformed cells, and the duration of the treatment is short, this should not be a cause for major concern.

3.2 VSV oncolysis of prostate cancer cells requires induction of autophagy

Induction of autophagy appears to be essential for HDIs to enhance VSV oncolytic activity. We have demonstrated this using autophagy-deficient MEFs, as well as a pharmacological inhibitor of autophagy in PC3 cells. In both cases, when autophagy was suppressed, HDIs were unable to increase VSV replication. In addition, when RelA/p65 was knocked down in PC3 cells, the effects of vorinostat on viral oncolysis and autophagy are strikingly reduced. These data provide evidence that HDI-mediated activation of NF- κ B stimulates autophagy, creating a cellular environment permissive to VSV replication and subsequent cell lysis. While the basis of this model appears to be at least partially due to autophagic inhibition of the antiviral response, other possibilities such as activation of ER stress or promotion of viral replication complexes cannot be excluded.

3.3 Concluding Remarks

OV combination therapy represents an auspicious new strategy in the war on cancer. Basic and clinical studies have both garnered encouraging results that could see these treatment modalities successfully treating patients in the near future. Thoroughly elucidating the mechanisms at work behind these therapies will be important in

selecting, adapting, and tailoring treatment strategies for particular cancers. In the case of VSV and HDI combination treatment, this study has contributed a bit more insight.

References

- Abaza MS, Bahman AM, Al-Attayah RJ, Kollamparambil AM. (2012). Synergistic induction of apoptosis and chemosensitization of human colorectal cancer cells by histone deacetylase inhibitor, scriptaid, and proteasome inhibitors: potential mechanisms of action. *Tumour Biol.* 33:1951-1972.
- Adam E, Quivy V, Bex F, Chariot A, Collette Y, Vanhulle C, et al. (2003). Potentiation of tumor necrosis factor-induced NF-kappa B activation by deacetylase inhibitors is associated with a delayed cytoplasmic reappearance of I kappa B alpha. *Mol Cell Biol* 23:6200–9.
- Ashburner BP, Westerheide SD, Baldwin Jr AS. (2001). The p65 (RelA) subunit of NF-kappaB interacts with the histone deacetylase (HDAC) corepressors HDAC1 and HDAC2 to negatively regulate gene expression. *Mol Cell Biol.* 21:7065– 77.
- Buerki, C., K. M. Rothgiesser, T. Valovka, H. R. Owen, H. Rehrauer, M. Fey, W. S. Lane, and M. O. Hottiger. (2008). Functional relevance of novel p300-mediated lysine 314 and 315 acetylation of RelA/p65. *Nucleic Acids Res.* 36:1665-1680.
- Chaturvedi, M.M., Sung, B., Yadav, V.R., Kannappan, R., Aggarwal, B.B. (2010). NF-kB addiction and its role in cancer: ‘one size does not fit all’. (2010). *Oncogene.* 1-16.
- Chen, L.F., Mu, Y., Greene, W.C. (2002). Acetylation of RelA at discrete sites regulates distinct nuclear functions of NF-kappaB. *Embo J.* 21:6539-6548.
- Dai, Y., Chen, S., Wang, L., Pei, X.Y., Funk, V.L., Kramer, L.B., Dent, P., Grant, S. (2011). Disruption of IkappaB kinase (IKK)-mediated RelA serine 536 phosphorylation sensitizes human multiple myeloma cells to histone deacetylase (HDAC) inhibitors. *J Biol Chem.* 286:34036-34050.
- Duan, J., Friedman, J., Nottingham, L., Chen, Z., Ara, G., Van Waes, C. (2007). Nuclear factor-kappaB p65 small interfering RNA or proteasome inhibitor bortezomib sensitizes head and neck squamous cell carcinomas to classic histone deacetylase inhibitors and novel histone deacetylase inhibitor PXD101. *Mol Canc Ther.* 6:37-50.
- Huang N, Katz JP, Martin DR, Wu GD. (1997). Inhibition of IL-8 gene expression in Caco-2 cells by compounds which induce histone hyperacetylation. *Cytokine.* 9:27–36.
- Inan MS, Rasoulpour RJ, Yin L, Hubbard AK, Rosenberg DW, Giardina C. (2000). The luminal short-chain fatty acid butyrate modulates NF-kappaB activity in a human colonic epithelial cell line. *Gastroenterology* 2000. 118:724–34
- Karin, M. (2006). Nuclear factor-kB in cancer development and progression. *Nature.* 441:431-436.

- Katsura T, Iwai S, Ota Y, Shimizu H, Ikuta K, Yura Y. (2009). The effects of trichostatin A on the oncolytic ability of herpes simplex virus for oral squamous cell carcinoma cells. *Cancer Gene Ther.* 16:237–45.
- Kiernan, R., V. Bres, R. W. Ng, M. P. Coudart, S. El Messaoudi, C. Sardet, D. Y. Jin, S. Emiliani, and M. Benkirane. (2003.) Post-activation turn-off of NF-kappa B-dependent transcription is regulated by acetylation of p65. *J Biol Chem* 278:2758-2766.
- Kirn, D. and Thorne, S. (2009). Targeted and armed oncolytic poxviruses: a novel multi-mechanistic therapeutic class for cancer. *Nat Rev Cancer.* 9:64.71
- Krämer OH, Göttlicher M, Heinzel T. (2001). Histone deacetylase as a therapeutic target. *Trends Endocrinol Metab.* 12:294–300.
- Nguyen TL, Abdelbary H, Arguello M, Breitbach C, Leveille S, Diallo JS, et al. (2008). Chemical targeting of the innate antiviral response by histone deacetylase inhibitors renders refractory cancers sensitive to viral oncolysis. *Proc Natl Acad Sci USA.* 105:14981–6.
- Orvedahl, A. and Levine, B. (2009). Autophagy in mammalian antiviral immunity. *Curr Top Microbiol Immunol.* 335:267-285.
- Otsuki A, Patel A, Kasai K, Suzuki M, Kurozumi K, Chiocca EA, et al. (2008). Histone deacetylase inhibitors augment antitumor efficacy of herpes-based oncolytic viruses. *Mol Ther.* 16:1546–55.
- Quivy V, Adam E, Collette Y, Demonte D, Chariot A, Vanhulle C, et al. (2006). Synergistic activation of human immunodeficiency virus type 1 promoter activity by NF-kappaB and inhibitors of deacetylases: potential perspectives for the development of therapeutic strategies. *J Virol.* 76:11091–103.
- Shen, H.M. and Codogno, P. (2011). Autophagic cell death: Loch Ness monster or endangered species? *Autophagy.* 7:457-465.
- Vanoosten RL, Earel Jr JK, Griffith TS. Enhancement of Ad5-TRAIL cytotoxicity against renal cell carcinoma with histone deacetylase inhibitors. (2006). *Cancer Gene Ther.* 13:628–32.
- Watanabe T, Hioki M, Fujiwara T, Nishizaki M, Kagawa S, Taki M, et al. (2006). Histone deacetylase inhibitor FR901228 enhances the antitumor effect of telomerase-specific replication-selective adenoviral agent OBP-301 in human lung cancer cells. *Exp Cell Res.* 312:256–65.
- White, E. (2012). Deconvoluting the context-dependent role for autophagy in cancer. *Nat Rev Cancer.* 12:401-410.
- Yao, J., Qian, C.J., Ye, B., Zhang, X., Liang, Y. (2012). ERK inhibition enhances TSA-induced gastric cancer cell apoptosis via NF-κB-dependent and Notch-independent mechanism. *Life Sci.* 91:186-193.